OVERVIEW AND ANALYSIS OF THE 29 DECEMBER 2006 TEXAS TORNADO OUTBREAK

Gregory R. Patrick, Ted Ryan, Stacie Hanes, Eric Martello, Jennifer Dunn

NOAA/National Weather Service
Weather Forecast Office
Fort Worth/Dallas, Texas

November 2009

Abstract

A tornado outbreak with a total of 26 reported tornadoes occurred across Texas on 29 December 2006. Twenty-two of the tornadoes occurred within the area of responsibility of the Fort Worth/Dallas Weather Forecast Office. This event was unprecedented with regard to the number of tornadoes that occurred during a single episode in north Texas in the month of December. The outbreak is documented by providing a brief overview of the tornadoes and tornado warnings, a discussion of the pre-storm environment on the synoptic scale, an analysis of the mesoscale and thermodynamic environment before and during the tornado occurrences, and a radar analysis of the most significant supercell storms. As a slow-moving, intense upper-level cyclone moved across the southwestern United States, an unseasonably warm and moist air mass spread north from the Gulf of Mexico into much of central and eastern Texas. Tornadic supercells developed near a warm front in an environment with steep mid-level lapse rates, moderate surface-based instability and extremely strong low-level vertical wind shear. All of the supercells developed well east of the occluded front and appeared to organize into several north-south oriented bands. Of the 22 tornadoes that were documented across north Texas, three were rated F2, with one fatality and damage estimates over $6 million.

1. Introduction

On 29 December 2006, a rare event unfolded in north Texas, as a tornado outbreak produced 22 tornadoes across the Fort Worth/Dallas (FWD) Weather Forecast Office (WFO) county warning area (CWA). The area that defines the FWD CWA is depicted in Fig. 1. Only two other wintertime tornado outbreaks have been documented across north Texas since 1950. The 29 December 2006 tornado outbreak produced more tornadoes than any other winter tornado outbreak case since 1948.

The potential for severe weather existed on 29 December 2006, as a powerful upper-level trough across the southwestern United States and northern Mexico moved slowly toward west Texas. An occluded front was progressing eastward across west Texas, with an east-west oriented warm front moving north through the eastern half of the state. As late as six hours prior to the onset of the outbreak, the pattern appeared to favor the development of a severe, linear convective system along the occluded front. However, tornadic supercell thunderstorms developed in several north-south bands east of the occluded front in a zone of pronounced low-level thermal advection.

Despite extensive cloud cover during the day, surface temperatures warmed within the zone of pronounced low-level thermal advection. Low-level winds remained strong from the southeast during the day in an environment characterized by intense vertical wind shear and large values of storm-relative helicity (SRH). The combination of high values of low-level convective available potential energy (CAPE) and large SRH values supported strong low-level mesocyclones and tornadic development. Of the 22 tornadoes that occurred in the FWD CWA, three were rated F2 on the legacy Fujita Scale, causing significant structural and tree damage, several injuries, and one fatality.

This paper examines the tornado outbreak on 29 December 2006 and explores the synoptic and mesoscale factors that combined to create this event. Section 2 provides an overview of the tornadoes including a detailed summary of the tracks and damage produced by the three F2 tornadoes. Section 3 reviews the synoptic pattern of the event and compares this event with other cold-season and warm-season tornadic episodes. Similarities and differences in the low-level and surface patterns with other cold-season tornado

events are also compared in Section 3. A comprehensive review of the mesoscale factors and thermodynamic environment that were critical to the outcome of this event are discussed in Section 4. Finally, Section 5 provides an in-depth radar analysis of the event and interrogation of the storms that produced the F2 tornadoes.

2. Damage Survey Results and Findings

Twenty-two of the 26 tornadoes that were reported across Texas on 29 December 2006 occurred across the FWD CWA, affecting 12 of the 46 counties that comprise the CWA. The tornado outbreak on this day was the largest across north Texas since 25 April 1994 when 24 tornadoes were reported in the FWD CWA. Verification statistics for Probability of Detection (POD) and False Alarm Ratio (FAR) (Schaefer 1990) are presented in Table 1.

Two local NWS survey teams were dispatched on 30 December and 31 December to survey the most significant areas of damage. These teams surveyed areas in Limestone, Coryell, Bosque, Hill, Johnson and Anderson Counties, finding evidence of tornado damage from eleven tornadoes in these six counties. The remaining tornadoes were rated based on pictures and information provided by emergency managers and county officials. Three strong tornadoes occurred and were all assigned F2 ratings, the highest Fujita rating confirmed on this day. Table 2 provides a summary of the three F2 tornadoes. These three tornadoes will be discussed in further detail in the following paragraphs. Of the remaining 19 tornadoes, five were rated F1 and 14 were rated F0. Figure 2 depicts the tracks of all 22 tornadoes across the FWD CWA.

The first F2 tornado of the day occurred in Limestone County and tracked approximately 32.2 km (20 mi). The tornado formed at 1942 UTC (142 PM CST), approximately 3.2 km (2 mi) north-northwest of Kosse. Early signs of damage were uprooted trees and minor damage to barns, sheds, and roofs. The tornado then struck a retirement home for veterans (Fig. 3a) approximately 6.4 km (4 mi) southwest of Groesbeck, where an elderly man lost his life and several others were injured. Much of the home was substantially damaged and portions of the roof were torn off. Other F2 damage occurred to a barn next to the veterans' home and to another barn down the road that was totally destroyed. As the tornado continued on its north-northeast track at

4

17 m s^{-1} (38 mph), it moved just west of Groesbeck where the tornado struck several more structures. Four homes sustained major damage and one wood-framed house partially collapsed. Numerous trees were also uprooted or snapped and several barns sustained major damage. Finally, the tornado dissipated as it moved into Fort Parker State Park. On average, this tornado was 0.36 km (400 yd) wide with estimated maximum wind speeds of 54 to 56 m s^{-1} (120 - 125 mph).

The second F2 tornado of the day developed at 2053 UTC (253 PM CST) in Bosque County, approximately 6.9 km (4.3 mi) east of Clifton. This tornado tracked to the north-northeast at 18 m s^{-1} (40 mph). It first struck a turkey farm causing significant damage, with debris scattered over 0.4 km (0.25 mile) from the farm. The tornado then tracked to the east of Womack, where it caused F2 damage (Fig. 3b) to two barns and minor damage to trees and fences in the same area. The tornado dissipated about 4.8 km (3 mi) northeast of Womack. The path of this tornado was approximately 11.4 km (7 mi) long, with an average width of 0.27 km (300 yd), and estimated maximum wind speeds of 60 m s^{-1} (135 mph). No injuries or fatalities resulted from this tornado.

The third and longest track F2 tornado of the day developed in northwestern Hill County and crossed into Johnson County before dissipating. This tornado developed at 2125 UTC (325 PM CST), approximately 6.4 km (4 mi) south of Blum. The parent supercell was the same supercell thunderstorm that produced the earlier F2 tornado in Bosque County. Taking a northeast track at a speed of 18 m s^{-1} (40 mph), the tornado entered Johnson County southeast of Rio Vista and dissipated at 2203 UTC (403 PM CST) near the south shore of Lake Alvarado. The path length was estimated to be about 36.5 km (22.7 mi). Widespread damage to trees, power poles, roofs, and windows was noted along the track. Indicators of F2 damage in Hill County included a large barn that was destroyed and a well-constructed home that was missing part of its roof decking. In Johnson County, 22 residences were destroyed (Fig. 3c), 20 more were heavily damaged, an additional 20 had minor damage, and several more structures suffered either partial or complete roof loss. Twelve people in Johnson County were injured with two sustaining serious injuries. On average, the tornado was 0.22 km (250 yd) wide,

but portions of the damage track indicated the tornado may have been as wide as 0.5 km (0.33 mi) at times. Estimated maximum wind speeds were around 60 m s^{-1} (135 mph).

Only a few reports of hail and flash flooding were received during the storms of 29 December 2006. Two separate occurrences of 2.2 cm (0.88 in) diameter hail were reported in Bell County from the same non-tornadic storm. The third report of hail was associated with the supercell that produced the F2 tornado in Johnson County. Hail up to 4.4 cm (1.75 in) diameter was reported as the tornadic storm moved through Cleburne, just west of the tornado's path. No other hail events were reported with any of the tornadic storms this day. Later in the evening of 29 December, continued heavy rainfall and training of convective cells led to flash flooding with several incidents reported across five counties. A seven year-old boy drowned after the car in which he was a passenger was overcome by high water in Freestone County.

Across the FWD CWA, two people lost their lives during this event and thirty-two more were injured. Total monetary damage from the entire event was estimated in *Storm Data* at $6.7M with $6.5M resulting from 20 of the 22 tornadoes (NCDC 2007). Other damages with monetary losses were caused by flash flooding, hail, thunderstorm winds, and lightning.

3. Synoptic Scale Evolution

Fawbush et al. (1951) made the first sketch of features common to severe thunderstorm outbreaks. Barnes and Newton (1983) further refined the model for the Great Plains (Fig. 4). In general, a strong mid-latitude trough is found in the upper levels of the atmosphere with a surface cyclone located downstream. A favorable orientation of upper-level jets plays a role in creating large scale upper-level divergence and enhancing vertical wind profiles.

The features described by Barnes and Newton are present regardless of whether the outbreak occurs in the warm or the cool season. For a tornado outbreak, which was defined by Galway (1977) as ten or more tornadoes, the presence of sufficient instability and favorable wind shear over a wide geographic region is required (Hamill et al. 2005). This section will present a synoptic analysis of the tornado outbreak that

occurred on 29 December 2006 and compare that synoptic pattern to those during other cold- and warm-season north Texas tornado outbreaks.

a. 29 December 2006 synoptic pattern

The synoptic scale pattern in the 48 hours preceding 29 December 2006 was dominated by a slow-moving closed low over the southwestern United States in the mid and upper levels of the atmosphere. By 1200 UTC 29 December, the low was accompanied by a cyclonically curved 250-hPa jet, with a maximum speed of 77 m s^{-1} (150 kt), extending from Nevada and southern California southeastward through northern Mexico and northeast into Texas (Fig. 5).

During the 24 hours preceding the tornado outbreak, the center of the large closed low at 500 hPa progressed slowly, moving only from Phoenix, Arizona to El Paso, Texas. The slow movement of the system resulted in the transport of unusually rich low-level moisture from the southeastern Gulf of Mexico, across a large part of the central United States from Texas into Minnesota (Fig. 6). At 0000 UTC 29 December, observed 850- and 925-hPa specific humidity anomalies were between 2 and 3 standard deviations above normal across north Texas. The moisture was carried north by persistent southerly and southeasterly 850-hPa and 925-hPa winds of 18-23 m s^{-1} (35-45 kt). By the morning of 29 December, mid-level lapse rates exceeded 8.0° C km^{-1}, likely owing to persistent differential temperature advection and the influence of synoptic-scale upward vertical motions acting to decrease static stability (Iribarne and Godson 1981). The low-level temperature and equivalent potential temperature (Θ_e) changes were most pronounced at 925 hPa, indicating the importance of this level for diagnosing convective instability and boundary layer moisture content prior to this tornado outbreak.

When the tornado outbreak was in its early stages at 1800 UTC 29 December 2006, surface dew points from 15° to 17°C (upper 50s to lower 60s °F) covered almost all of north Texas, with the richest moisture located just south of an advancing warm front where 18°C (64 °F) dew points were spreading into the region. Precipitable water values (Fig. 7) were over 3.6 cm (1.4 in) at the time of the outbreak, which is over two

standard deviations above normal for December (Bunkers 2007) and illustrates the anomalously high moisture content.

Cool-season tornado outbreaks typically feature very strong vertical wind shear, in addition to weak or marginally adequate surface-based instability (Guyer et al. 2006). The wind profile on 29 December 2006 was no exception, as strong directional and speed shear was present through a deep layer of the troposphere east of the upper-level cyclone. Magnitudes and trends in vertical wind shear are discussed in greater detail in Section 4.

b. Other North Texas cool-season outbreaks

Galway and Pearson (1981, hereafter GP81) analyzed tornado outbreaks occurring in the winter months (December, January, and February). They found a total of 16 winter tornado outbreaks across the Great Plains between 1950 and 1979. Since tornadoes are relatively rare across north Texas in the winter, the definition of a tornado outbreak as defined by Galway (1977) was modified for this paper to include events with seven or more tornadoes, instead of ten or more. Even with this adjusted criterion, only two other winter tornado outbreaks were found in north Texas since 1950. There was one other significant case on 18 February 1971 with five tornadoes within FWD's CWA and another three just outside the CWA but still within Texas. The February 1971 case will be analyzed as a significant cool-season tornado event, but will not be labeled an outbreak.

Besides 29 December 2006, the two other winter tornado outbreaks analyzed include 14 December 1971 and 17 January 1996. In the December 1971 case, there were 19 tornadoes in north Texas, causing 25 injuries and $14.2M in damages. There were only seven tornadoes associated with the January 1996 case with a total of $1.8M in damages.

A 500-hPa mean pattern of cool season tornado outbreaks presented by GP81 (Fig. 8a) shows a full-latitude open-wave trough with a slight negative tilt, extending from Montana to New Mexico. The 500-hPa pattern during the December 1971 case (Fig. 8b) featured a powerful, yet fast-moving southern stream shortwave. This case was most similar to the mean pattern, except that the base of the upper-level trough was

located slightly farther north and east. The cases from February 1971 (Fig. 8c) and January 1996 (Fig. 8d) also showed some similarities except that the troughs were broader. The main shortwave affecting north Texas during the January 1996 event was in the southern stream, similar to the December 1971 case, although this shortwave remained aligned with the mean trough to the north.

The case in December 2006 (Fig. 8e) was different than the others because it featured a strong closed low centered farther south over extreme southern New Mexico and northern Mexico and greater 500-hPa geopotential height values. The December 2006 case is the only one which featured a slow-moving upper-level closed low, rather than an open wave or progressive upper-level trough.

The mean 850-hPa chart presented by GP81 (Fig. 9a) is similar to the 850-hPa patterns for the December 1971, February 1971, and January 1996 (Figs. 9b-9d) events. The 850-hPa pattern analyzed from the December 2006 case (Fig. 9e) is unique in that heights were much higher than all other cases and the GP81 mean. In addition, the 850-hPa low center was located much farther south and was likely responsible for the south-southeast winds, as opposed to the south-southwest flow depicted in the GP81 mean and the other three cases.

Convective instability is often limited during the winter months, and the presence of a conditionally unstable boundary layer is generally needed for tornado outbreaks. In this study we assessed values and changes in Θ_e at 925 hPa as a means for comparing boundary layer destabilization trends of the four events. All three tornado outbreak cases had 925-hPa Θ_e values greater than 330 K during the time of the tornado outbreak, while the 12-hour change in Θ_e was between 8 K and 14 K (Fig. 10). During the February 1971 event, there was only a small 12-hour change in Θ_e (2-4 K across north Texas) with Θ_e values only around 320 K.

GP81 also developed a mean surface low pressure track for wintertime tornado outbreak-producing systems across the Great Plains (red line in Fig. 11), which showed a surface low forming in the western Texas Panhandle before tracking east and then northeast across central Oklahoma and into the Midwestern states. The surface low tracks for the four winter tornado outbreak cases studied in north Texas are similar to the GP81 mean track, although they are generally located slightly farther north. It is interesting to note that the primary

surface low with the 29 December 2006 case tracked farther south than any of the other cases and just south of the GP81 mean. The central pressures of the surface cyclones for the four winter cases varied greatly. The surface cyclone during the December 1971 outbreak had a central pressure of 996 hPa while the January 1996 outbreak cyclone had a central pressure of 984 hPa and the February 1971 case was only 999 hPa. Since the 850-hPa heights were also relatively high for the December 2006 outbreak, it is not surprising that the primary surface cyclone with the 2006 outbreak also had the highest surface pressure of the four cases at 1008 hPa. At least two mesoscale areas of low pressure (mesolows) developed across Texas south of the primary surface cyclone during the 2006 event. These mesolows are discussed in Section 4.

c. Comparisons to warm-season outbreaks

Eleven springtime cases were chosen as a means to compare a "typical" spring outbreak with the three winter outbreaks. The most notable difference was that upper-level and surface cyclones were usually weaker for spring outbreaks, and sometimes displayed little to no seasonal anomalies.

The eleven spring cases could be split into two sub-categories. The first category featured a well-defined upper-level trough over the western United States (Fig. 12a) with some similarities to the winter outbreak pattern shown by GP81. The other sub-category of spring tornado outbreaks was associated with a less-amplified upper-level pattern, more subtle upper-level features (Fig. 12b), and transient surface lows whose movements were influenced by diabatic heating. Although subtle upper-level features may imply weaker forcing, three of the five subtle forcing cases displayed significant low-level warm and theta-e advection at 850 hPa and 925 hPa. Maddox and Doswell (1982) suggested that in the absence of classic synoptic-scale forcing features, intense low-level warm advection can compensate to generate severe convection.

The plot of surface lows and their tracks (Fig. 13) indicates the tendency for lows to be located in the Texas Panhandle and west Texas at the time of the tornado outbreaks across north Texas. Springtime surface lows were often slower moving than their wintertime counterparts, as depicted by the significantly shorter lines.

Note that the springtime plot of surface lows from large dynamic systems displayed the most variance, with tracks often well displaced from north Texas.

4. Thermodynamic and Mesoscale Environment

This section assesses the thermodynamic environment and kinematic profiles across north Texas during the December 2006 tornado outbreak. The focus will be on the evolution of the mesoscale environment in a diagnostic sense.

a. Evolution of Thermodynamic Environment

The atmospheric environment in the early morning hours of 29 December 2006 was characterized by widespread low cloud cover, gusty southeast surface winds, unseasonably warm temperatures, high relative humidities, and scattered light showers. The 1200 UTC surface analysis (not shown) indicated a surface low in the Texas Panhandle, with an occluded front extending south across west and southwest Texas.

The 1200 UTC sounding from Fort Worth TX (KFWD) is shown in Fig. 14. The thermodynamic profile featured a nearly saturated layer from the surface to near 700 hPa. A strong inversion is noted near 700 hPa, with lapse rates of 8.2°C km^{-1} between 700 hPa and 300 hPa. East-southeast winds of 7 m s^{-1} (15 kt) veer to southeasterly and increase to 21 m s^{-1} (40 kt) at 1 km AGL. Winds become southerly at 800 hPa (1.8 km AGL) and gradually increase to 26 m s^{-1} (50 kt) at 500 hPa before veering to south-southwest at 46 m s^{-1} (90 kt) near 250 hPa. A 2- m temperature of 16.6° C (62° F) and dew point of 13.0° C (55° F) at observation time led to negligible low-level surface-based CAPE (SBCAPE) values on the 1200 UTC KFWD sounding.

A proper diagnosis of the morning environment should include an assessment of nearby or upstream profiles of temperature, moisture, and wind to aid in the evaluation of important gradients that may act to modify the atmospheric environment later in the day. Given the deep-layer southerly flow in the 1200 UTC KFWD sounding, a suitable site for that assessment was Corpus Christi TX (KCRP; Fig. 15). Table 3 summarizes thermodynamic and wind shear parameters from 1200 UTC soundings taken at both KFWD and

KCRP. Comparison of the observed parameters at these two sites indicates that both temperature lapse rates and vertical wind shear values were similar on the two soundings. One noticeable difference was in low-level moisture with KCRP's sounding exhibiting substantially higher low-level mixing ratios.

It was surmised in the morning that low-level cloud cover would inhibit diabatic heating and that convective destabilization via low-level warm, moist advection would be a relatively slow process. Low-level cloud cover was indeed persistent in many areas during the day of 29 December 2006, but very strong low-level winds aided in significant warming and moistening of the low levels across the southern part of the FWD CWA.

b. Surface Boundaries and Mesoscale Environment

Indications early in the day suggested that the eastward progressing occluded front would provide the primary mesoscale focus for strong to severe thunderstorms, possibly in the form of a squall line or a quasi-linear convective system. The Storm Prediction Center (SPC) Day 1 Convective Outlook, shown in Fig. 16, also mentioned that the potential for linear mesoscale convective system (MCS) development was supported by strong meridional flow, east of the intense upper-level trough located to the west, with mean wind vectors nearly parallel to the north-south oriented frontal boundary. However, the occluded front was not a direct, major factor in the tornado outbreak as numerous supercell thunderstorms developed east of this frontal boundary. The potential for discrete supercells and tornadoes in pre-frontal convection was mentioned in the SPC Day 1 outlook at 1257 UTC, but the highest tornado probabilities were assigned in southeast Texas.

Rich low-level moisture, steep lapse rates, and low-level thermal advection are believed to be the primary characteristics that contributed to the development of widespread convection on 29 December 2006. By 1800 UTC, a mesoscale surface low pressure center (mesolow) had developed along the occlusion point of the cold front and a warm front, the latter extending across the extreme southern part of the FWD CWA (Fig. 17). The warm front was associated with only a subtle change in wind direction but was analyzed based on a temperature gradient on the order of $5°$ C $(100 \text{ km})^{-1}$. Many of the tornadic storms initiated in the zone of low-

level warm advection in the vicinity of (but not necessarily on) the northward-moving surface warm front during the afternoon hours. All of the tornadic supercells occurred east of the occluded front.

The hodograph based on winds from the National Oceanic and Atmospheric Administration Profiler Network site at Palestine, TX (PATT2) at 1800 UTC is shown in Fig. 18. Since the surface warm front was analyzed (see Fig. 17) just south of the Palestine wind profiler site at 1800 UTC, the wind profiler data and derived shear parameters are thought to be representative of the environment near and just north of the surface warm front. The 10 m - 1 km shear value on the PATT2 hodograph is 17 m s^{-1} (34 kt), which is similar to that observed on the 1200 UTC KFWD sounding and illustrated that intense low-level environmental shear persisted into the afternoon.

Figure 19 shows selected mesoanalysis graphics, produced by SPC (see Bothwell et al. 2002) at 1500 UTC, 1800 UTC, and 2100 UTC. Surface dew points over 15.6° C (60° F) overspread much of north Texas during the day, and a surface thermal ridge became established roughly parallel to and east of the occluded front. At 850 hPa, 21 to 26 m s^{-1} (40 to 50 kt) south-southeasterly flow was persistent during the day as 10°C and higher dew points spread as far north as the Red River bordering Oklahoma. Low-level environmental wind shear, as measured by the magnitude of the 10 m - 1 km shear vectors, increased during the day with values up to 21 m s^{-1} (40 kt) analyzed across the southeast part of the FWD CWA by 2100 UTC.

By 2200 UTC, the surface mesolow was analyzed northwest of Stephenville, TX (KSEP), and the warm front extended east-southeast to just north of Palestine (Fig. 20). Some relatively weak convection had developed along the occluded front and the cold front, but more intense, supercellular convection was occurring in several linear north-south oriented clusters east of the mesolow.

Significant surface pressure falls were observed across much of north Texas during the afternoon hours. Figure 21 illustrates the magnitude and extent of the pressure falls, which were maximized at 2000 UTC over the eastern half of the FWD CWA with values over 4 hPa (3 h)$^{-1}$. The extent and magnitude of the surface pressure falls across north Texas were likely a testament to the strong and sustained low-level thermal advection east of the surface mesolow.

Figure 22 shows a skew-T plot from KFWD at 0000 UTC 30 December 2006 that has been modified in the low levels to better represent the thermodynamic environment of storms near or south of the warm front. A surface temperature/dew point of 21.1°/17.0° C (70/63° F) was used to modify the lowest levels of the sounding. Table 4 shows some derived parameters associated with the modified sounding in Fig. 22. The helicity calculations given in the table were based on a storm movement of 193° at 17 m s^{-1} (33 kt), which is approximately the average radar-observed storm motion for the right-moving, tornadic supercells during this event.

c. Discussion

Given the favorable values of instability and the intense vertical wind shear concentrated in the lowest 1 km AGL, it is not difficult to explain the occurrence of numerous supercell thunderstorms and tornadoes. Values of several of the parameters shown in Table 4 are within the range of values correlated with environments favoring significant tornadoes (Davies 2002; Hart and Korotky 1991; Rasmussen 2003; Rasmussen and Blanchard 1998). Persistent east or east-southeast winds in the near-surface layer maximized environmental shear and helicity on both sides of the warm front throughout the event.

One noteworthy aspect of this tornado outbreak was that high values of surface – 3 km CAPE interacted effectively with ambient low-level vertical shear to augment ascent and vortex stretching through the nonhydrostatic pressure field (Rotunno and Klemp 1982; Rasmussen 2003). In his study of 321 supercell profiles, Davies (2002) found that profiles associated with supercell tornadoes tended to have more low-level CAPE than those associated with non-tornadic supercell events. Given the strong low-level vertical wind shear, the relatively large area analyzed with low-level CAPE values in excess of 100 J kg^{-1} (Fig. 23) was believed to be a primary contributor to the tornado outbreak.

Convective initiation east of the occluded front and the ability of supercells to remain discrete in an environment characterized by numerous convective clusters are two aspects of this event worth mentioning. Certainly, the forcing for large-scale ascent in the form of sustained and strong low-level warm advection

14

created a favorable convective environment for development. Strong winds near and just above the surface contributed to atmospheric destabilization through horizontal thermal and moisture advection.

Thunderstorm initiation was widespread in this environment with most of the significant supercell thunderstorms having origins either in a surface Θ_e ridge or in a zone of surface Θ_e advection. Figure 24 depicts the origins of two significant thunderstorms around 1800 UTC. One storm appeared to initiate in the Θ_e advection maximum south of the surface warm front (see Fig. 17) and the other storm appeared to initiate very close to the surface warm front. Radar-derived storm scale trends of both tornadic supercells are discussed in Section 5.

Convective initiation and the apparent tendency for the most significant storms to organize into north-south bands oriented parallel to the mean wind or shear vector are topics worthy of additional study. Although some of the significant convection appeared to initiate near the warm front (see Figs. 17 and 20), origins of most convective cells could not be tied directly to the warm front.

Figure 25 illustrates the convective organization banding that was observed during the event. At several times during the outbreak, there appeared to be a tendency for significant convective development to occur in bands that were approximately evenly spaced. There are several plausible explanations for the presence of evenly spaced convective bands oriented parallel to the mean wind or shear vectors east of the mesolow and occluded front. Enhanced zones of mesoscale lift near low-level jet maxima, the presence of subtle mesoscale convergence boundaries, or topographically induced waves downstream of Mexico's Sierra Madres could possibly explain the observed trends in convective organization.

5. Radar Analysis of Tornadic Supercells

The primary warning decision tools used by forecasters during the tornado outbreak were two network Weather Surveillance Radar – 1988 Dopplers (WSR-88Ds). Specifically, the radar sites for Fort Worth/Dallas (KFWS) and for Fort Hood (KGRK) were used extensively by WFO FWD forecasters due to their proximity to severe convection. The locations of these radars in relation to the FWD CWA are shown in Fig. 1. This

section will analyze reflectivity and velocity features related to storm structure and their importance to the warning decisions. In particular, two tornadic supercells which produced the three F2 tornadoes were chosen for detailed analysis and discussion. The initiation regions of both supercells were shown in Fig. 24.

a. Limestone County Tornadic Supercell

The convective cell that evolved into the Limestone County supercell initiated shortly after 1800 UTC near a maximum in surface Θ_e advection across Burleson County (see Fig. 24). The initial cell intensified rapidly into a supercell thunderstorm as it moved north-northeast from Robertson County into Limestone County after 1935 UTC. Based on analysis of KGRK WSR-88D data, the average storm top (maximum height of 30-dBZ return) during the tornadic phases of the supercell was 10.2 km (33.5 kft) with a mesocyclone diameter averaging 4.0 km (2.2 nm).

Prior to and during its tornadic phase, the Limestone County supercell exhibited several notable radar indications of a thunderstorm with an intense rotating updraft. In addition to persistent and deep cyclonic signatures associated with the mesocyclone, reflectivity signatures of a strong updraft were present. A bounded weak echo region (BWER; Lemon and Doswell 1979) was well-defined on the 1940 UTC volume scan from KGRK (Fig. 26). The F2 tornado produced by this storm started at 1942 UTC. The BWER structure became less defined as the storm tracked north of Groesbeck after 2000 UTC; a diminishing updraft or increased distance from KGRK may have contributed to loss of radar-indicated BWER. The storm produced a second tornado (F0) northwest of Mexia in the far northeast portion of Limestone County. The supercell thunderstorm continued northeast, crossing the warm front (see Figs. 17 and 20), then weakening as it encountered a more stable environment north of the warm front.

Algorithm output from KGRK WSR-88D Radar Product Generator (see Klazura and Imy 1993) was used to analyze trends in rotational velocity of the Limestone County supercell between 1916 UTC and 2019 UTC. Figure 27 is a time series chart of the magnitude of rotational velocity of the Limestone County supercell. The trends in shear values appear to confirm that the timing and life cycle of the strong low-level

16

mesocyclone coincided with tornadogenesis. Note the peaks in shear values at 1935 UTC and 2010 UTC that precede reported tornado occurrences in each instance. This finding is similar to that discussed in a Grant and Prentice (1996) study of supercells where maxima in values of low-level rotational velocity were observed prior to tornadogenesis.

b. Coryell, Bosque, Hill, and Johnson Counties' Cyclic Tornadic Supercell

A long-lived supercell thunderstorm initiated near the surface warm front prior to 1900 UTC (see Figs. 20 and 24), producing several tornadoes across Coryell, Bosque, Hill, and Johnson Counties. This supercell thunderstorm produced the longest-track tornado of the day, affecting parts of Hill and Johnson Counties between 2125 UTC and 2203 UTC (see Fig. 2).

This particular supercell thunderstorm can be characterized as 'cyclic' during its lifetime, as new updrafts and subsequent mesocyclones formed along rear-flank gust fronts (Burgess et al. 1982). In cyclic supercell thunderstorms, circulations become occluded and eventually dissipate as rear-flank outflow eventually cuts off moist inflow into the low-level mesocyclone.

Decisions to issue tornado warnings for this supercell were aided by WSR-88D signatures of strong cyclonic rotation. Several well-defined rotation signatures and small-scale hook echoes were evident during mesocyclone intensification. Figures 28 and 29 show the radar depiction of the supercell across Hill County and Johnson County at the time the F2 tornado was occurring.

The low-level circulation may have been enhanced by storm-scale interactions with weaker convective cells near Itasca, Texas (see Fig. 28). The resulting tornado crossed into southeast Johnson County and dissipated near Alvarado at 2203 UTC, as the parent supercell encountered an increasingly more stable low-level environment and inversion north of the warm front. The tornadic storm was best analyzed from KGRK in the early stages through 2000 UTC before moving into better sampling from KFWS during latter stages of tornadic development. Figure 30 depicts trends in rotational velocity with this supercell.

c. Relationship of Mesoscale Factors to Tornadogenesis

The exact influence of the warm front, as it related to low-level mesocyclogenesis and tornadogenesis, is unclear. Instability and low-level vertical wind shear were both favorable for the development of supercells on either side of the warm front. However, a cursory analysis suggests that circulations of both supercell thunderstorms analyzed in this section appeared to strengthen when they encountered the enhanced low-level horizontal vorticity that was likely associated with the surface warm front. The tornado occurrence across Johnson County around 2200 UTC is evidence that conditions favorable for tornadoes were present in areas immediately north of the analyzed position of the warm front at 2200 UTC (see Fig. 20).

6. Summary

An anomalous synoptic pattern combined with a moist and unstable low-level environment to support a rare winter tornado outbreak across north Texas on 29 December 2006. As an upper-level low deepened over the Desert Southwest, warm air advection at the surface transported a warm and moist airmass from the Gulf of Mexico. Twenty-two tornadoes touched down in the WFO FWD CWA, with three assigned a F2 rating. Only two other wintertime tornado outbreaks have been documented in north Texas, and the outbreak on 29 December 2006 was the largest of the three.

An analysis of the synoptic pattern on this day revealed an upper-level trough and surface low that both tracked farther south than the average Great Plains winter tornado outbreak pattern as determined by Galway and Pearson (1981). This system was different from previous winter outbreaks in that the upper-level trough developed a closed circulation. Local analyses prior to and during the event showed a surface occluded front moving towards north Texas from the west, while a subtle warm front moved north through the eastern half of the state. Prognoses from as late as six hours prior to the event were that a convective line would develop along the occluded front, then progress eastward as a linear MCS during the day. Instead, discrete, tornadic supercells developed in evenly spaced, north-south bands east of the occluded front in a zone of low-level warm advection.

Low-level features on 29 December 2006 were important to the outcome of the event, as the tornado outbreak occurred east of the region of synoptic-scale, upper-level forcing for upward vertical motion. The environment north of the warm front was already unstable with steep mid-level lapse rates, abundant moisture, and strong low-level and deep-layer shear. However, the environment near the warm front was instrumental in further increasing the low-level instability to support tornadic development and possibly enhancing low-level shear profiles. Supercells developed east of the occluded front with the tornadic storms moving to the north-northeast at speeds up to 20 m s^{-1}. Traditional supercell radar signatures of strong updrafts and strong low-level mesocyclones were observed during the event, leading to a POD of over 91% for tornado events across north Texas.

This case represents a rare event where attention to detail regarding anomalous synoptic-scale features and mesoscale analyses were crucial in determining storm mode. The anomalous southern track of the dynamic upper-level system and its slow movement allowed for an unseasonably moist and unstable low-level environment to spread into north Texas from the Gulf of Mexico days before the tornado outbreak.

References

Albers, S. C., J. A. McGinley, D. L. Birkenheuer, and J. R. Smart, 1996: The Local Analysis and Prediction

System (LAPS): Analyses of clouds, precipitation, and temperature. *Wea. Forecasting,* **11,** 273–287.

Barnes, S. L., and C. W. Newton, 1983: Thunderstorms in the synoptic setting. *Thunderstorm Morphology and*

Dynamics, E. Kessler, Ed., Vol. 2, *Thunderstorms: A Social, Scientific, and Technological*

Documentary, University of Oklahoma Press, 75–112.

Bothwell, P. D., J. A. Hart, and R. L. Thompson, 2002: An integrated three-dimensional objective analysis

scheme in use at the Storm Prediction Center. Preprints, *21st Conf. Severe Local Storms*, San Antonio,

TX, Amer. Meteor. Soc., J117-J120.

Bunkers, M., 2007: "Precipitable Water Plots". National Weather Service Forecast Office, Rapid City, SD.

[Available online at http://www.crh.noaa.gov/unr/?n=pw].

Burgess, D. W., Wood, V. T., and Brown, R.A., 1982: Mesocyclone evolution statistics, Preprints, *12th Conf.*

on Severe Local Storms, San Antonio, TX, Amer. Meteor. Soc., 422-424.

_____, R. R. Lee, S. S. Parker, D. L. Floyd, and D. L. Andra, 1995: A study of mini supercells observed by

WSR-88D radars. Preprints, *27th Conf. on Radar Meteorology,* Vail, CO, Amer. Meteor. Soc., 4-6.

Davies, J. M., 2002: On low-level thermodynamic parameters associated with tornadic and non-tornadic

supercells, Preprints, *21st Conf. on Severe Local Storms,* San Antonio, TX, Amer. Meteor. Soc., 603-606.

Fawbush, E. J., R.C. Miller, and L.G. Starrett, 1951: An empirical method of forecasting tornado development.

Bull. Amer. Meteor. Soc., **32**, 1-9.

Galway, J. G., 1977: Some climatological aspects of tornado outbreaks. *Mon. Wea. Rev.*, **105**, 477-488.

_____, and A. Pearson, 1981: Winter tornado outbreaks. *Mon. Wea. Rev.*, **109**, 1072-1080.

Grant, B., and R. Prentice, 1996: Mesocyclone characteristics of mini supercell thunderstorms. Preprints, *15th Conf. On Weather Analysis and Forecasting*, Norfolk, VA, Amer. Meteor. Soc., 363-365.

Guyer, J. L., D. A. Imy, A. Kis, and K. Venable, 2006: Cool season significant (F2-F5) tornadoes in the Gulf Coast states. Preprints, *23rd Conf. Severe Local Storms*, St. Louis, MO, Amer. Meteor. Soc., CD-ROM, 4.2.

Hamill, T. M., R. S. Schneider, H. E. Brooks, G. S. Forbes, H.B. Bluestein, M. Steinberg, D. Meléndez, and R.M. Dole, 2005: The May 2003 extended tornado outbreak. *Bull. Amer. Meteor. Soc.,* **86**, 531-542.

Hart, J. A., and W. Korotky, 1991: The SHARP workstation v1.50 users guide. National Weather Service, NOAA, U.S. Department of Commerce, 30 pp. [Available from NWS Eastern Region Headquarters, 630 Johnson Ave., Bohemia, NY 11716]

Iribarne, J. V., and W. L. Godson, 1981: *Atmospheric Thermodynamics.* D. Reidel Publishing Company, 259 pp.

Klazura, G. E., and D. A. Imy, 1993: A description of the initial set of analysis products available from the NEXRAD WSR-88D system. *Bull. Amer. Meteor. Soc.*, **74**, 1299-1300.

Lemon, Leslie R., and C. A. Doswell III, 1979: Severe thunderstorm evolution and mesocyclone structure as related to tornadogenesis, *Mon. Wea. Rev.*, 107, 1184-1197.

Maddox, R. A., and C. A. Doswell, 1982: An examination of jet stream configurations, 500 mb vorticity advection and low-level thermal advection patterns during extended periods of intense convection. *Mon. Wea. Rev.*, 110, 184–197.

McGinley, J. A., 1995: Opportunities for high resolution data analysis, prediction, and product dissemination within the local weather office. Preprints, *14th Conf. on Weather Analysis and Forecasting,* Dallas, TX, Amer. Meteor. Soc., 478–485.

NCDC 2007. *Storm Data*. Vol 48, No 12. [Available from National Climatic Data Center, 151 Patton Ave., Asheville, NC 28801-5001].

Rasmussen, E.N., 2003: Refined supercell and tornado forecast parameters. *Wea. Forecasting,* **18**, 530-535.

_____, and D. O. Blanchard, 1998: A baseline climatology of sounding-derived supercell and tornado forecast parameters. *Wea. Forecasting*, **13**, 1148-1164.

Rotunno, R., and J. B. Klemp, 1982: The influence of the shear-induced pressure gradient on thunderstorm motion. *Mon. Wea. Rev.,* **110**, 136-151.

Schaefer J. T., 1990: The critical success index as an indicator of warning skill. *Wea. Forecasting*, **5**, 570–575.
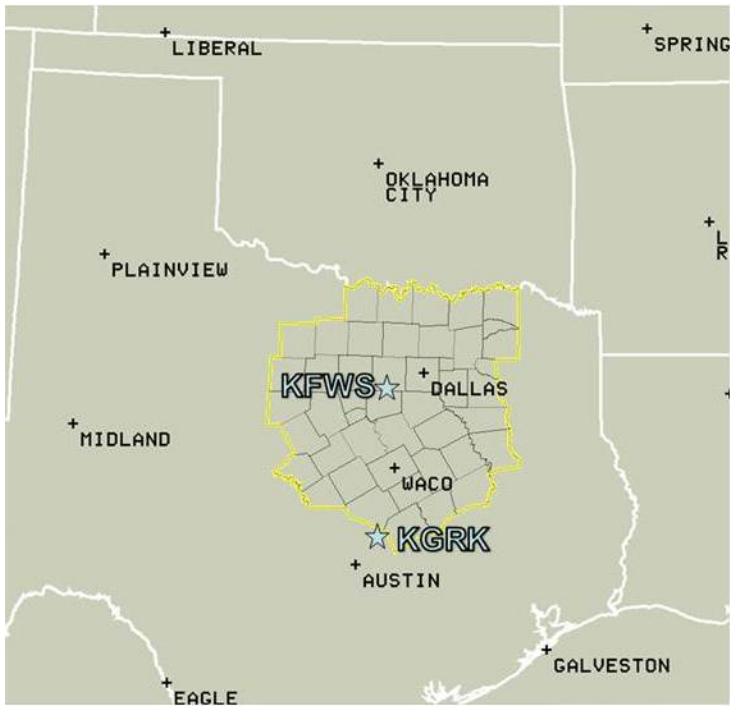
Fig. 1. Map highlighting the CWA of WFO FWD. Solid white lines are state outlines with city names in black text. The FWD CWA is outlined in yellow and is comprised of 46 counties across north and central Texas. Weather Surveillance Radar – 1988 Doppler (WSR-88D) locations for Dallas/Fort Worth (KFWS) and Fort Hood (KGRK) are highlighted with blue stars.
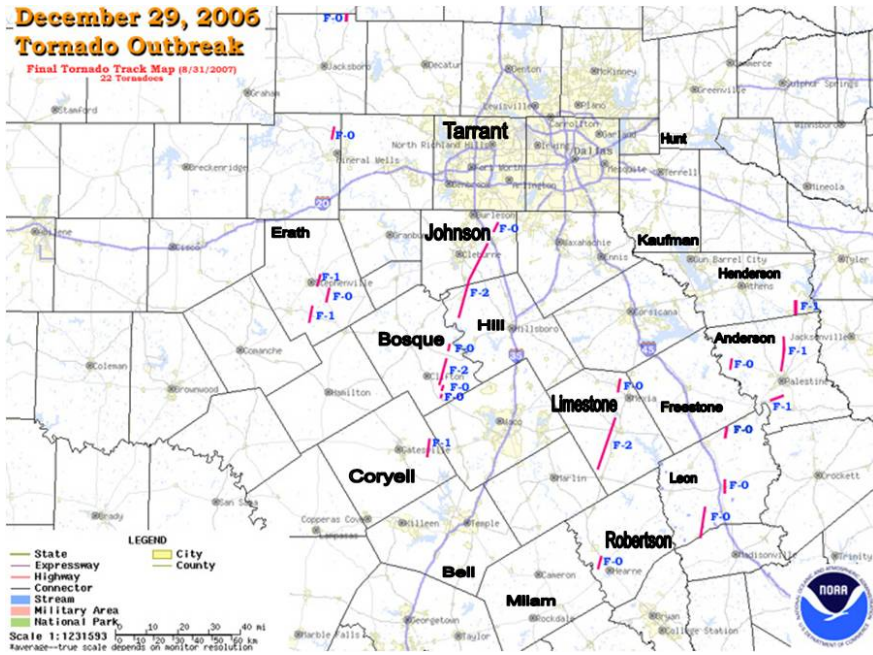
Fig. 2. Tracks of all 22 documented tornadoes in the WFO FWD CWA on 29 December 2006 based on Storm Data (NCDC 2007). Red lines give locations of tornado tracks; blue text near the tracks gives F-scale ratings assigned to each tornado. Bold black text gives names of counties mentioned in text.

Fig 3. Photographs of damage caused by tornadoes on 29 December 2006. (a) Significant damage to a retirement home for veterans located outside of Groesbeck in Limestone County; (b) Damage to a metal framed barn east of Clifton in Bosque County; c) Remains of a mobile home destroyed by a tornado northeast of Rio Vista in Johnson County (Photo courtesy Gerald Mohr, Johnson County Emergency Management Coordinator).
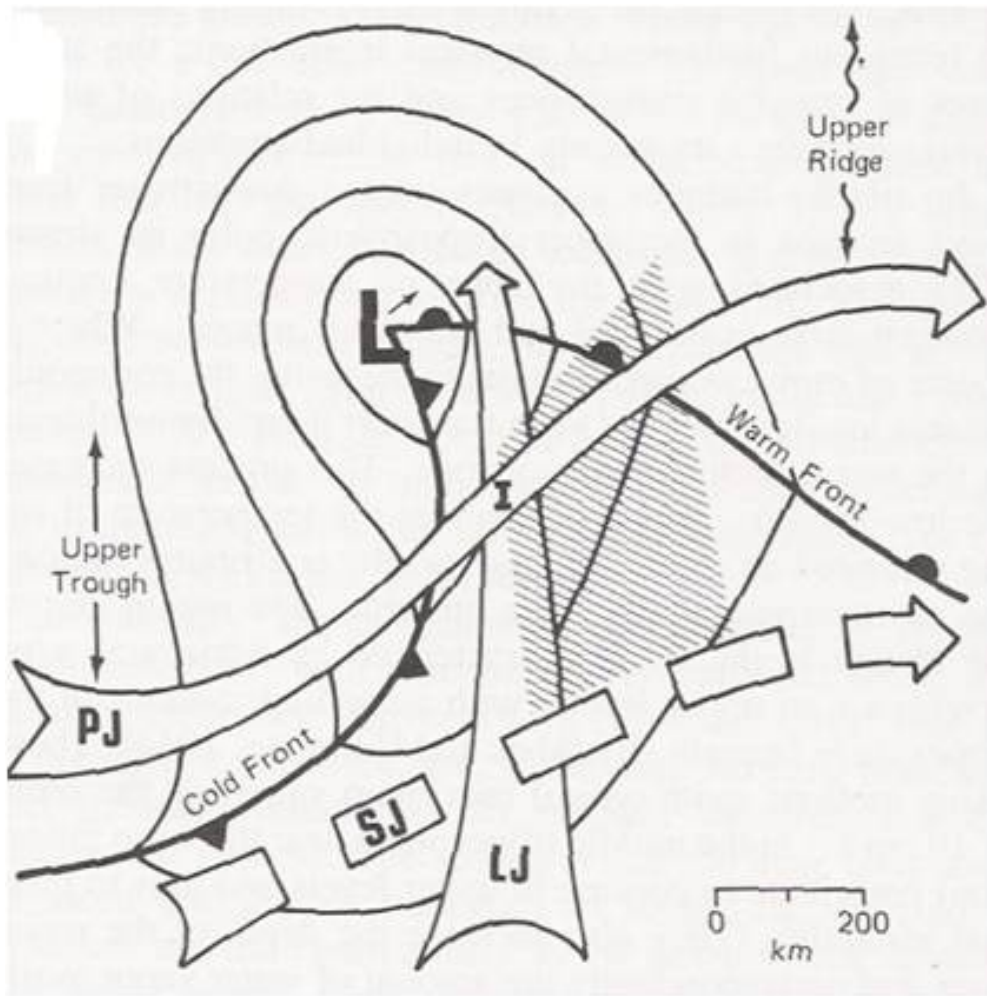
Fig. 4. Features common to severe weather outbreaks in the Great Plains, from Barnes and Newton (1983). These include an upper level trough, strong surface low, warm and cold fronts, and jets at several levels. The hatched area indicates the general area for severe weather, including tornadoes.
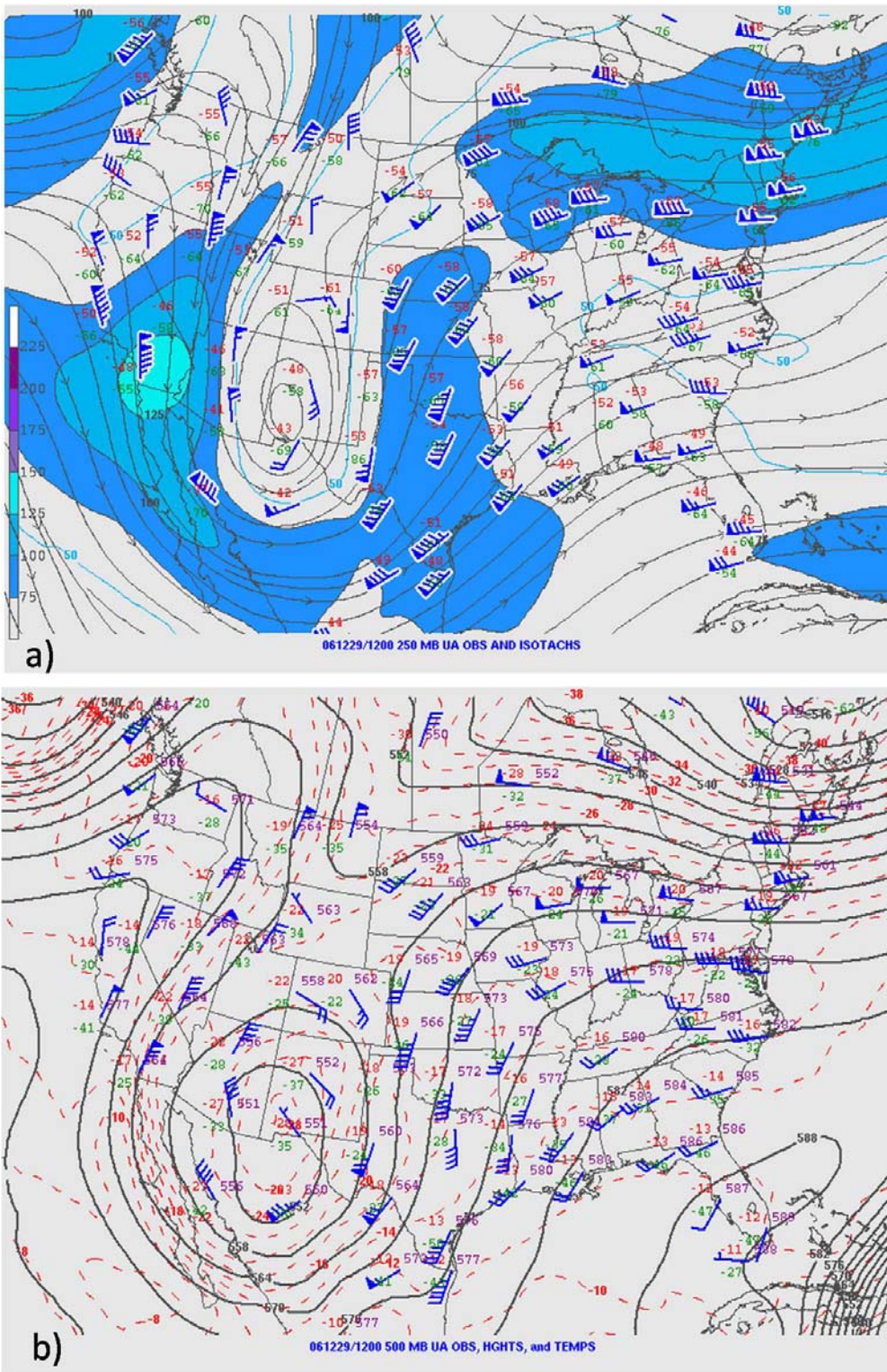
Fig. 5. Objectively analyzed upper-air charts for 1200 UTC 29 December 2006. Plotted observations of wind (blue barbs in knots), temperature (red numbers in C), and dew point (green numbers in C) are shown. (a) Analysis at 250 hPa with streamlines shown as solid gray lines and blue shaded region depicting analyzed wind speeds over 38 m s^{-1} (75 kt); (b) analysis at 500 hPa with constant geopotential heights analyzed with solid black lines and temperatures analyzed with dashed red lines. (Both images courtesy SPC).
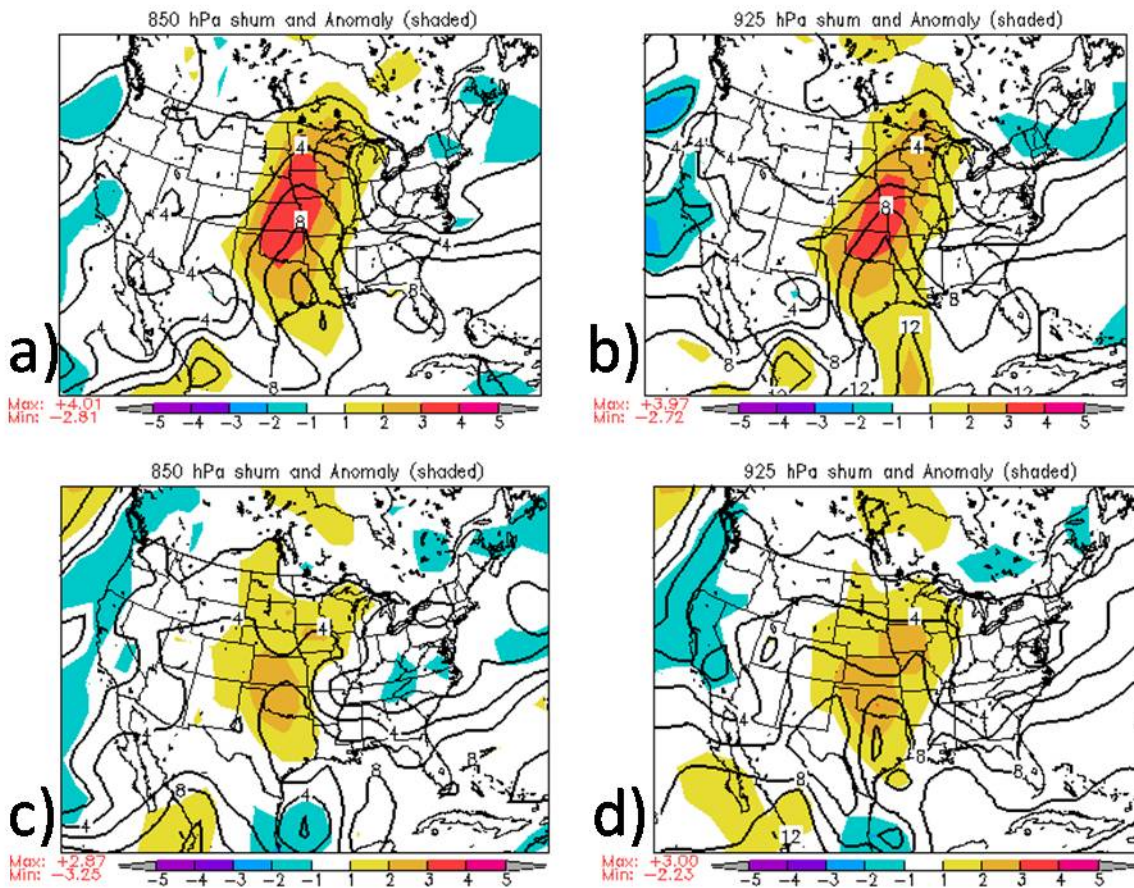
Fig. 6. Specific humidity values (contours g kg^{-1}) and standardized anomaly values (shaded) at (a) 850 hPa on 0000 UTC 29 December 2006, (b) 925 hPa on 0000 UTC 29 December, (c) 850 hPa on 0000 UTC December 30, and (d) 925 hPa on 0000 UTC December 30.
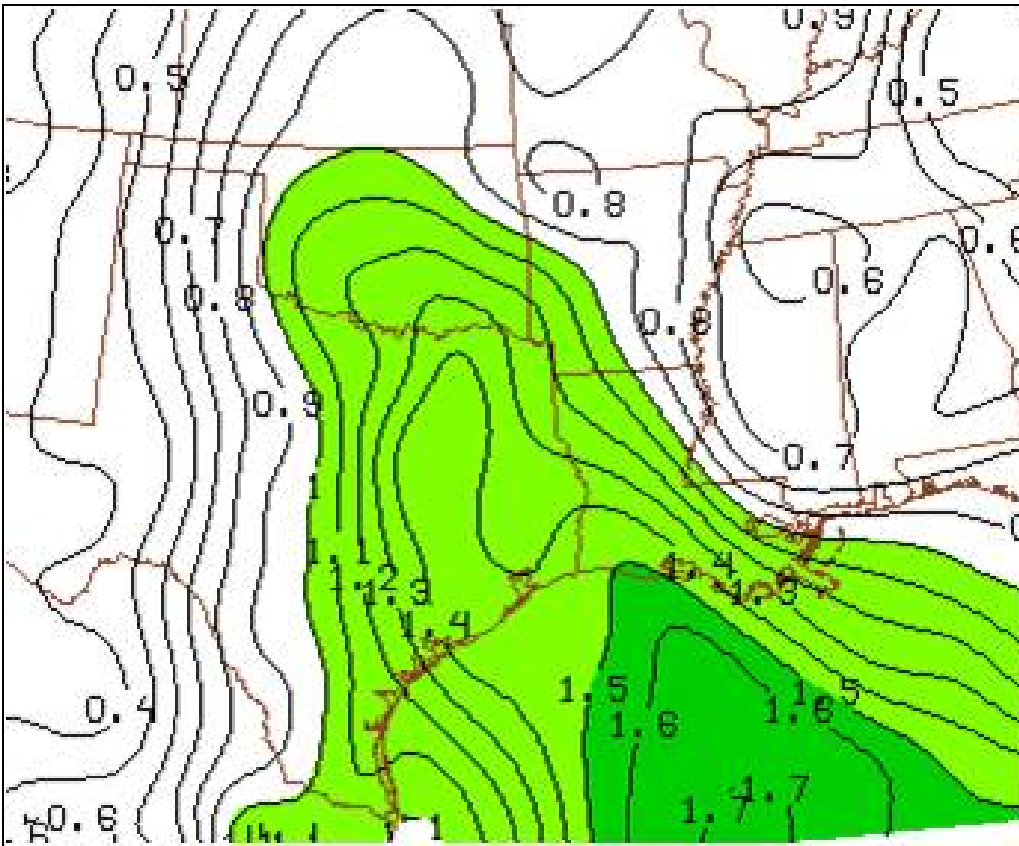
Fig. 7. Precipitable water values (in) across the southern U.S. at 0000 UTC 30 December 2006. Contours are drawn at 0.1 in. intervals. Light green shading represents values from 1.00 - 1.49 in while darker green shading represents values of 1.50 in and higher. (Courtesy SPC)
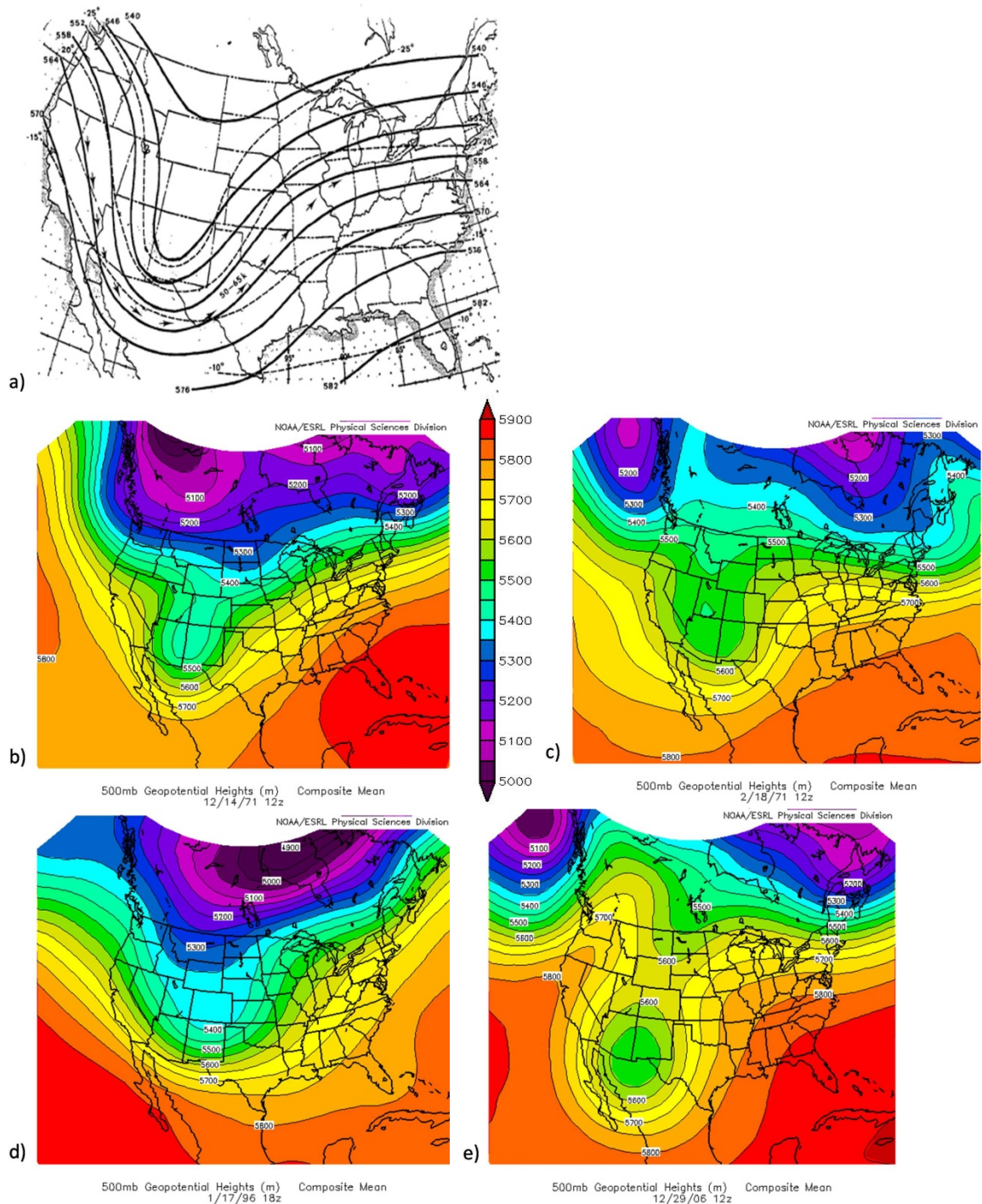
Fig. 8. Geopotential height contours at 500 hPa for (a) the average Great Plains winter tornado outbreak, from Galway and Pearson (1981), with solid lines indicating isohypses in dm, dashed lines indicating isotherms in °C, and arrows depicting location of wind maxima in kt; (b) the 14 December 1971 outbreak at 1200 UTC; (c) the 18 February 1971 case at 1200 UTC; (d) the 17 January 1996 outbreak at 1800 UTC; (e) the 29 December 2006 outbreak at 1200 UTC. Colored areas in b) – e) represent geopotential height values (m) corresponding to the scale shown. (b – e courtesy of NOAA/ESRL Physical Sciences Division)
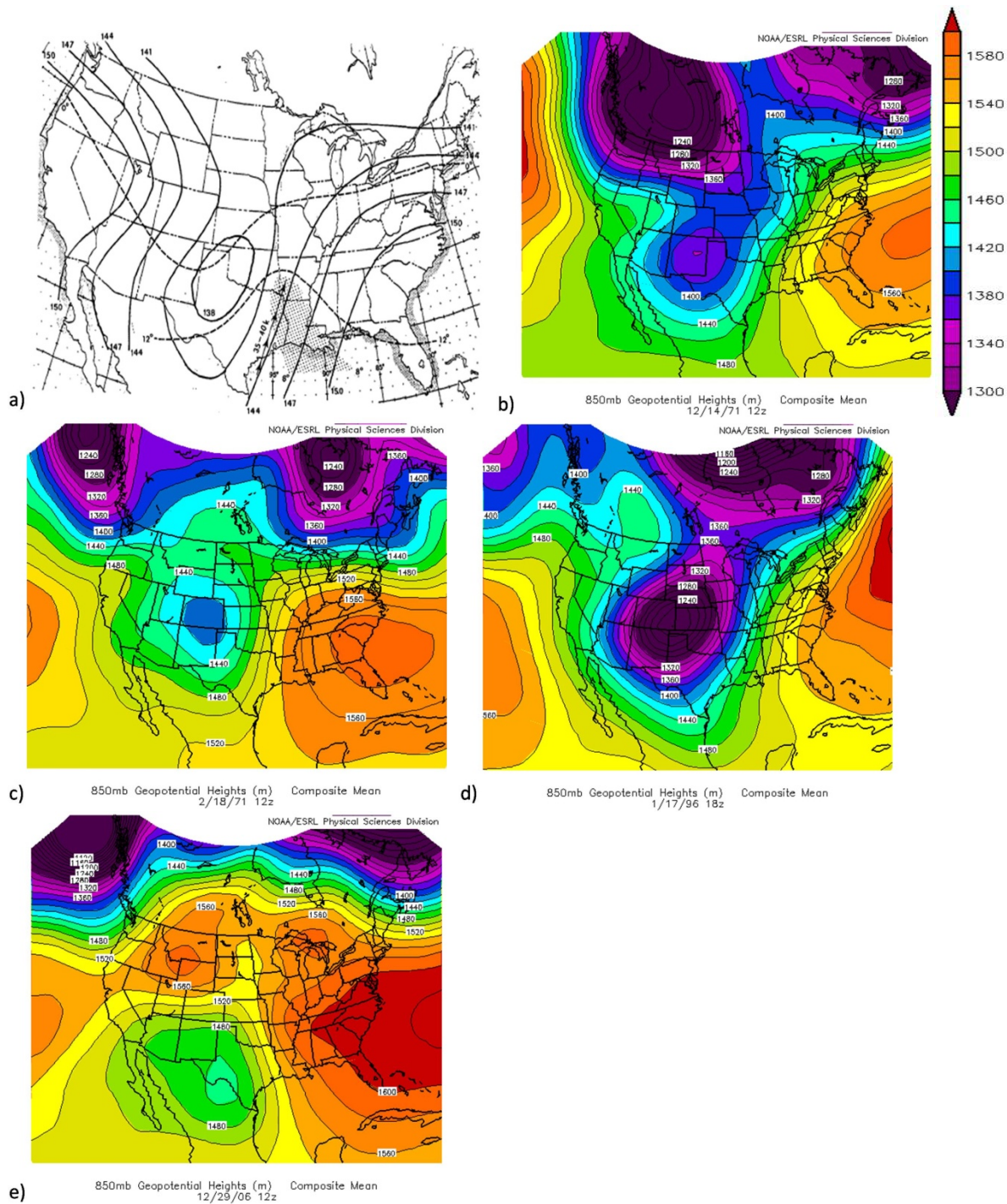
Fig. 9. Geopotential height contours at 850-hPa for (a) the average Great Plains winter tornado outbreak; from Galway and Pearson (1981), with solid lines indicating isohypses in dm, dashed lines indicating isotherms in °C, arrows depicting location of wind maxima in kt, and stippled region indicating 8° C or greater dew point temperatures; (b) the 14 December 1971 outbreak at 1200 UTC; (c) the 18 February 1971 event at 1200 UTC; (d) the 17 January 1996 outbreak at 1800 UTC; (e) the 29 December 2006 outbreak at 1200 UTC. Colored areas in b) – e) represent geopotential heights (m) corresponding to the scale shown. (b – e courtesy of NOAA/ESRL Physical Sciences Division)
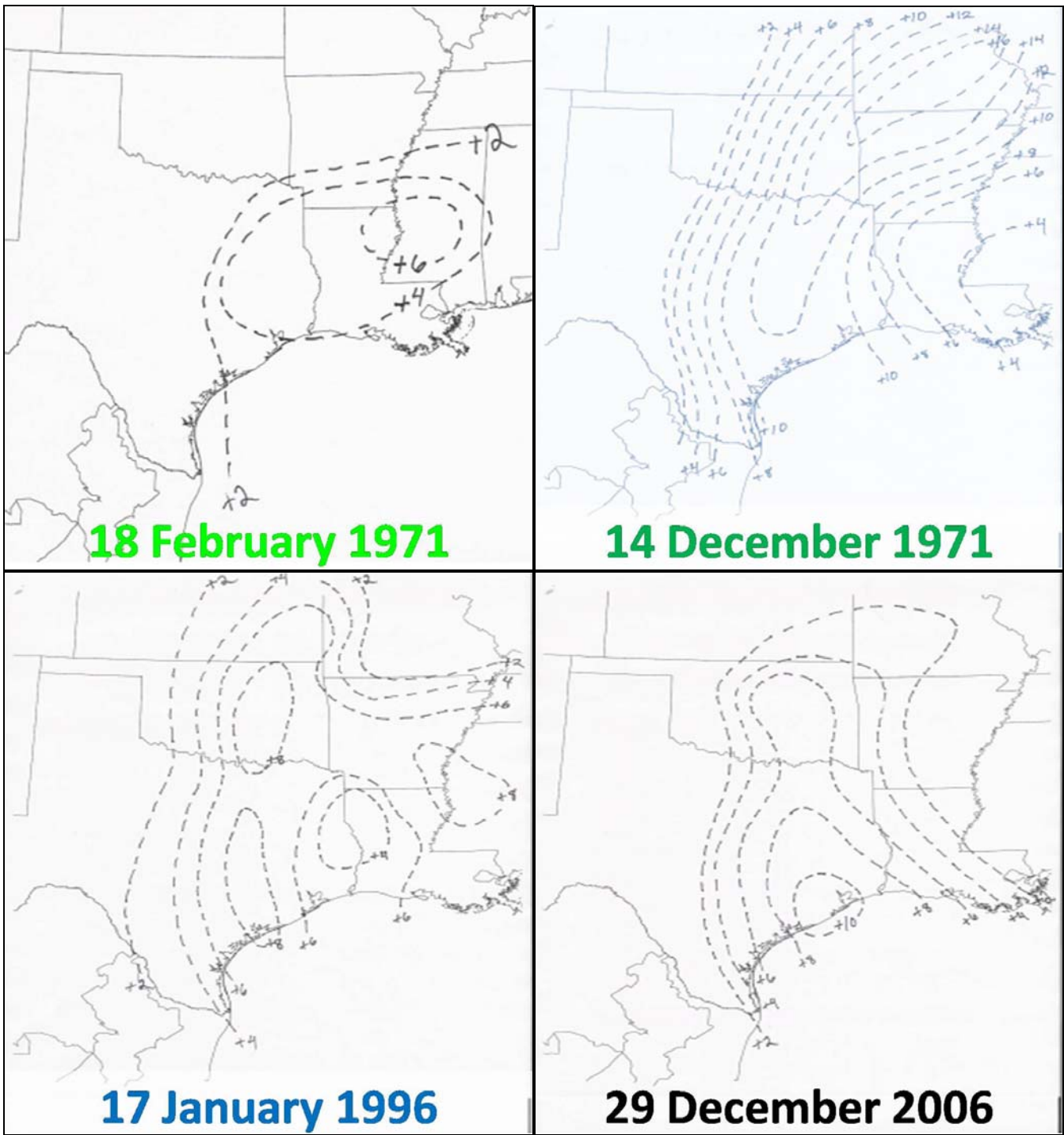
Fig. 10. Twelve-hour changes in equivalent potential temperature (Θ_e, K) at 925 hPa for the period ending at the time of the tornado events on the dates shown.
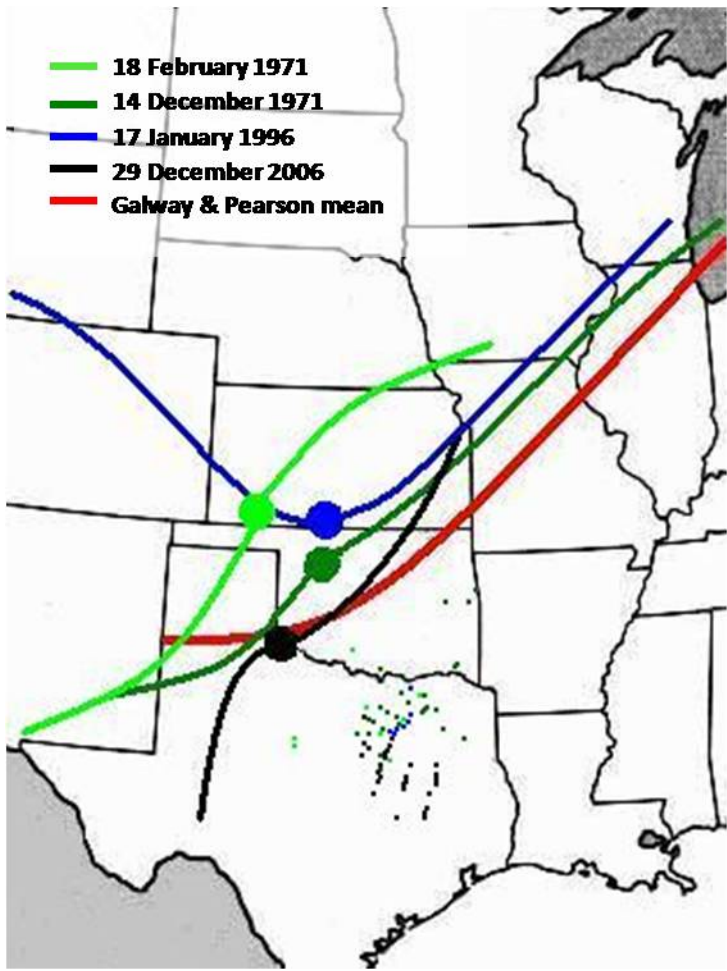
Fig. 11. Surface low tracks of four north Texas tornado events and mean winter outbreak track (red line) from Galway and Pearson (1981). Filled circles indicate the primary surface low position at the time of the tornado events. The individual tornadoes tracks are shown as dots. Their color indicates with which outbreak they are associated.
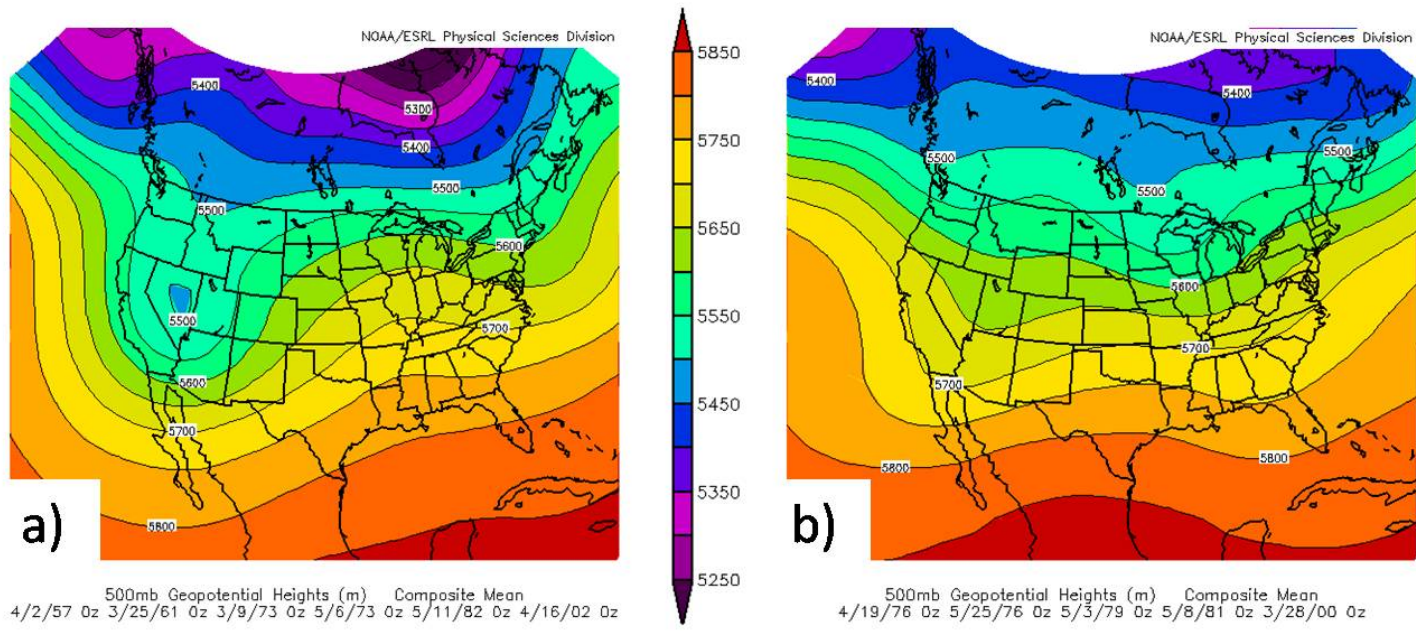
Fig. 12. Composite mean 500-hPa geopotential heights for warm season tornado outbreaks. (a) Composite of six events with amplified dynamics, and (b) composite of five events with subtle dynamics. The dates are listed as part of Fig. 13.
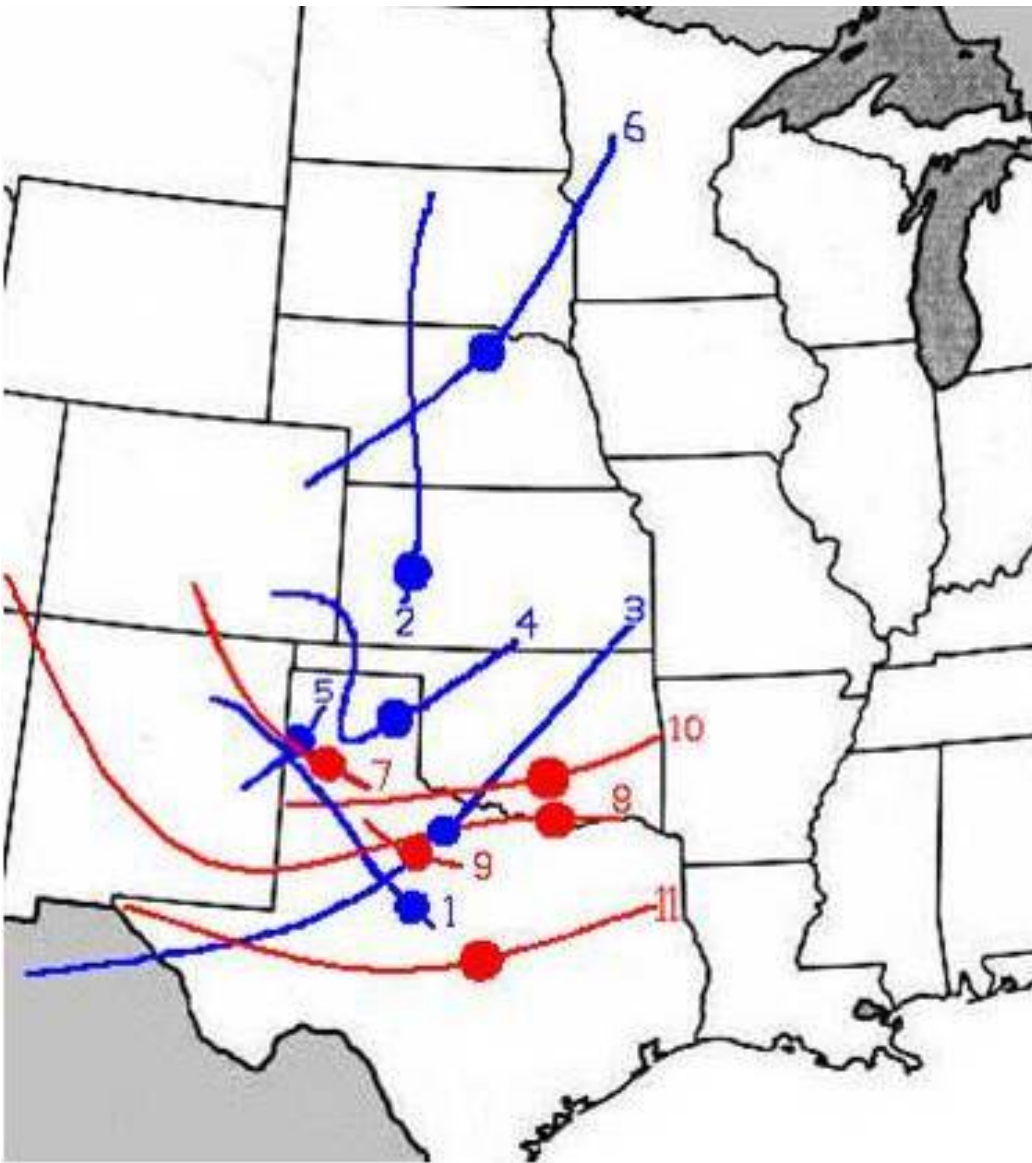
Fig. 13. Map showing surface low tracks one day before to one day after selected north Texas spring tornado outbreaks. The circles represent the location of the surface lows at the time of the outbreak. The blue lines are amplified dynamics events, and the red lines are the subtle dynamics events. Numbers represent the following cases:

Amplified Dynamics	Subtle Dynamics
1 : 2 April 1957	**7** : 19 April 1976
2 : 25-26 March 1961	**8** : 25-26 May 1976
3 : 9-10 March 1973	**9** : 3 May 1979
4 : 6 May 1973	**10** : 8-9 May 1981
5 : 11-12 May 1982	**11** : 28 March 2000
6 : 16 April 2002	
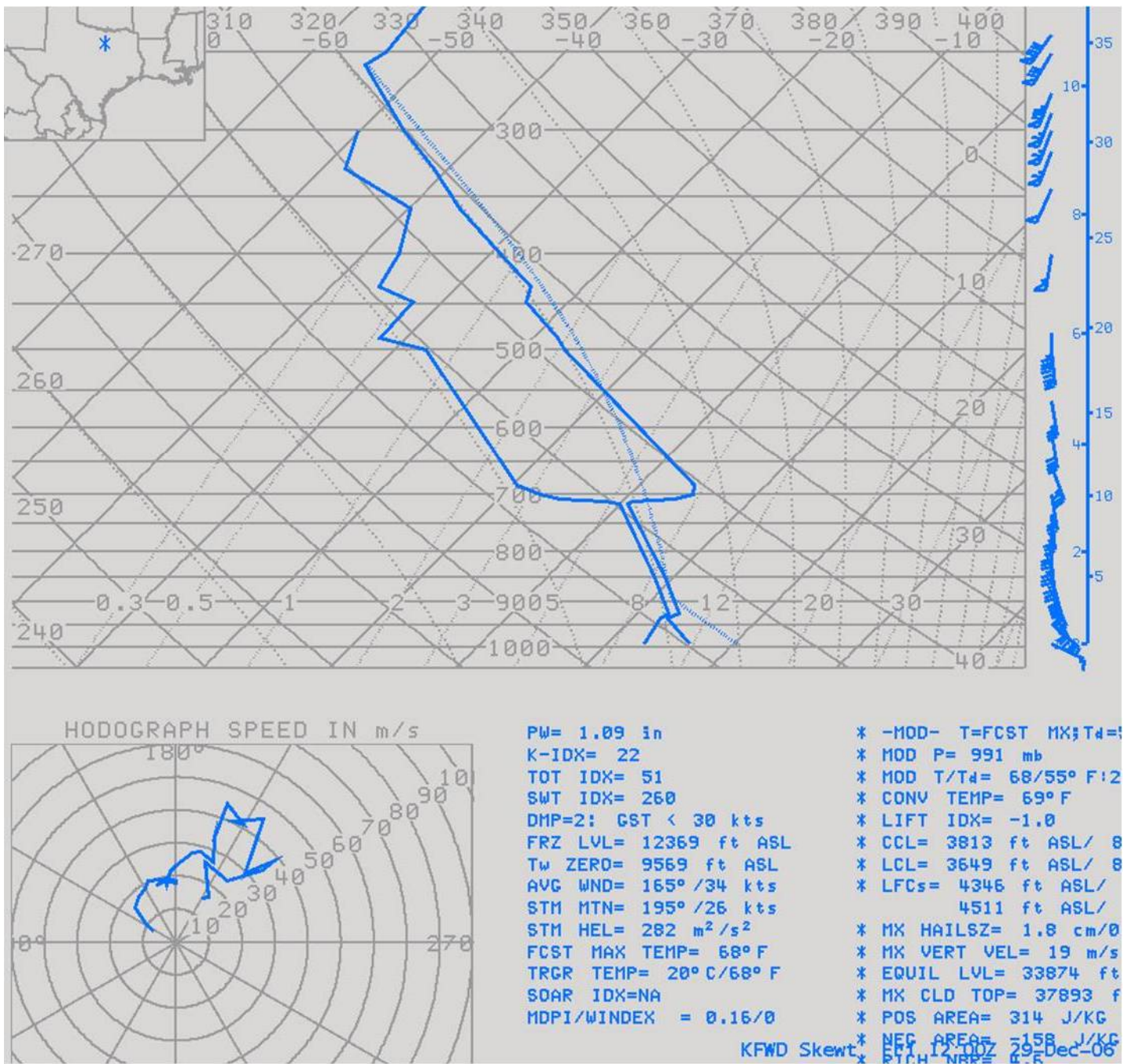
Fig. 14. Observed skew T-log p sounding of temperature and dew point from Fort Worth TX (KFWD) at 1200 UTC 29 December 2006. Note nearly saturated low levels and steep lapse rates between 685 hPa and 260 hPa. The calculated mean lapse rate between the top of inversion (685 hPa) and tropopause (258 hPa) is 8.4 °C km^{-1}.
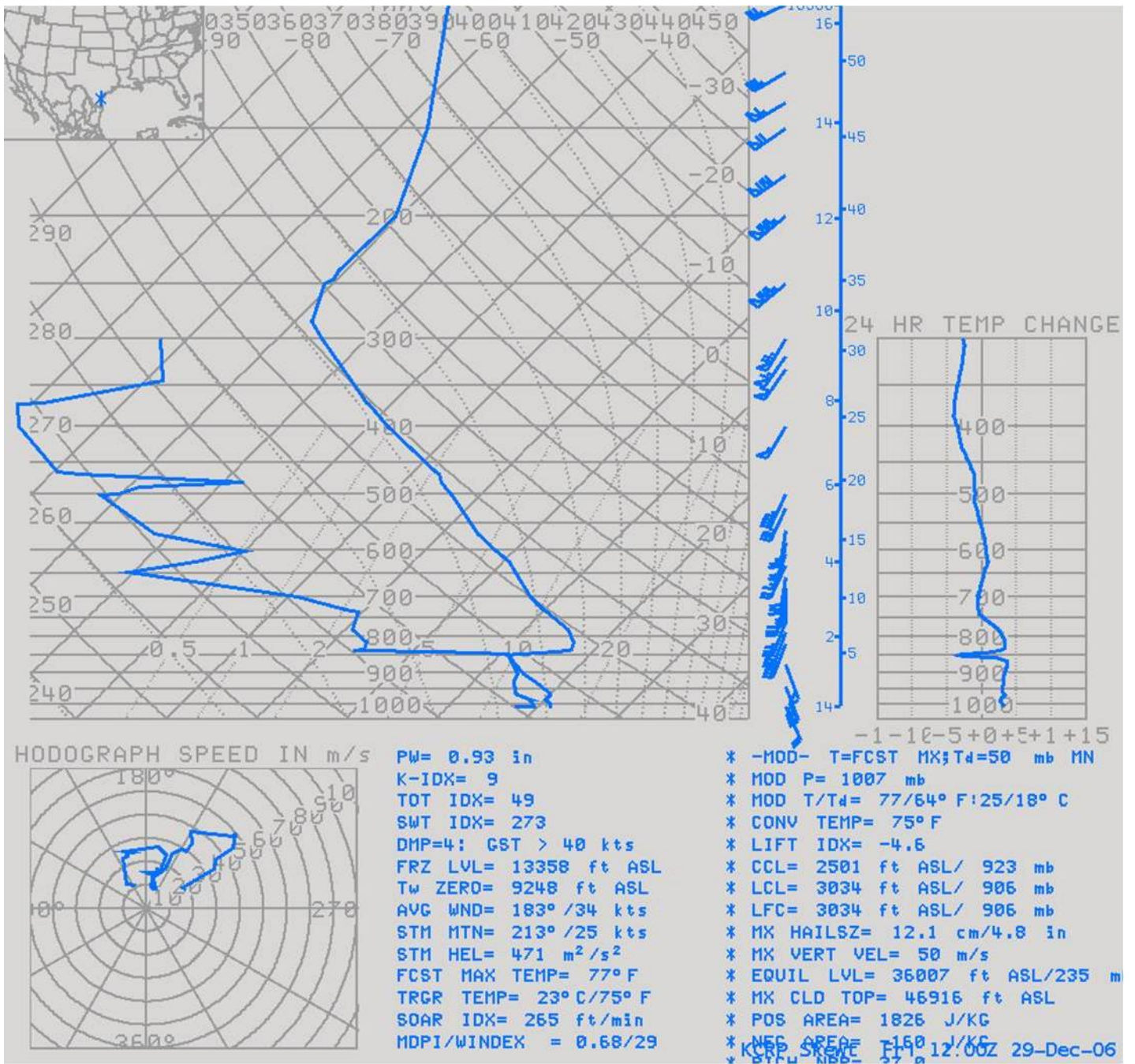
Fig. 15. Observed skew T-log p sounding of temperature and dew point from Corpus Christi TX (KCRP) at 1200 UTC 29 December 2006.

DAY 1 CONVECTIVE OUTLOOK
NWS STORM PREDICTION CENTER NORMAN OK
0657 AM CST FRI DEC 29 2006

VALID 291300Z - 301200Z

...THERE IS A SLGT RISK OF SVR TSTMS ACROSS CENTRAL/E TX TODAY INTO
E TX/WRN LA OVERNIGHT...

...CENTRAL AND E TX THROUGH EARLY SATURDAY...
A DEEP CLOSED LOW OVER SW NM THIS MORNING WILL MOVE SLOWLY EWD INTO
W TX BY EARLY SATURDAY...AS ONE OR MORE EMBEDDED SPEED MAXIMA ROTATE
NEWD/NWD AROUND THE ERN PERIPHERY OF THE LOW FROM THE MIDDLE RIO
GRANDE VALLEY INTO NW TX. AT THE SURFACE...A WEAK LOW WILL DEVELOP
SLOWLY EWD/NEWD FROM THE SE TX PANHANDLE INTO WRN OK...WHILE A COLD
FRONT SWEEPS EWD ACROSS CENTRAL TX BY THIS EVENING AND E TX
OVERNIGHT. THIS SURFACE BOUNDARY WILL PROVIDE THE PRIMARY FOCUS FOR
STRONG/SEVERE THUNDERSTORM DEVELOPMENT TODAY INTO TONIGHT ACROSS
CENTRAL AND E TX.

RECENT SURFACE/BUOY OBSERVATIONS AND GOES PW IMAGERY SUGGEST A SURGE
OF RICHER MOISTURE IS SPREADING NWWD ACROSS THE WRN GULF TOWARD THE
TX COAST.   THUS...BOUNDARY LAYER DEWPOINTS WILL LIKELY INCREASE INTO
THE MID-UPPER 60S ACROSS THE MIDDLE AND LOWER TX COASTAL PLAIN
TODAY...WITH DEWPOINTS NEAR 60 F EXPECTED AS FAR N AS I-20.   THE
STRONGER SURFACE HEATING WILL OCCUR TODAY IN THE PRE-FRONTAL WARM
SECTOR ACROSS S CENTRAL AND CENTRAL TX...WHERE AFTERNOON MLCAPE
VALUES SHOULD RANGE FROM 500 J/KG N TO NEARLY 2000 J/KG S.   THIS
INSTABILITY WILL SUPPORT AN EXPANDING BAND OF THUNDERSTORMS ALONG
THE FRONT FROM CENTRAL INTO NW TX BY LATER THIS AFTERNOON...WITH THE
FEED OF LOW-LEVEL MOISTURE MAINTAINED FROM S INTO CENTRAL TX BENEATH
THE PRONOUNCED CAP SHOWN IN THE 12Z CRP AND BRO SOUNDINGS.   GRADUAL
EROSION OF THE CAP IS EXPECTED BY THIS EVENING AS CONVECTION
DEVELOPS SWD INTO S TX AND CONTINUES EWD ACROSS S/SE OK AND E TX.

THE DEEP LAYER FLOW AND SHEAR VECTORS ARE FORECAST TO BE ORIENTED
LARGELY PARALLEL TO THE SURFACE FRONT ACROSS TX...THUS CONVECTION
WILL TEND TOWARD A LINEAR MODE ON THE MESOSCALE.   HOWEVER...VERTICAL
SHEAR WILL STILL BE SUPPORTIVE OF SUPERCELL STRUCTURES WITHIN THE
LARGER CONVECTIVE BAND...AND INCREASING MOISTURE/WEAKENING CIN MAY
ALLOW FOR MORE DISCRETE PRE-FRONTAL CONVECTION ACROSS SE TX.   A FEW
TORNADOES WILL BE POSSIBLE...ESPECIALLY BY TONIGHT ACROSS E/SE TX
WHERE AT LEAST WEAK SURFACE-BASED INSTABILITY WILL COINCIDE WITH A
50 KT LLJ AND 0-1 KM SRH IN EXCESS OF 300 M2/S2.   OTHERWISE...LARGE
HAIL AND DAMAGING WINDS CAN BE EXPECTED WITH THE STRONGEST STORMS
THIS AFTERNOON/EVENING ACROSS CENTRAL/S CENTRAL TX...AND THE
DAMAGING WIND THREAT WILL PERSIST TONIGHT ACROSS E TX IN WRN LA NEAR
THE END OF THE PERIOD.

..THOMPSON.. 12/29/2006

Fig. 16. Text of Day 1 Severe Weather Outlook issued at 1257 UTC 29 December 2006 by Storm Prediction Center. Highlighted sentences in first and third paragraphs are discussed in the text.
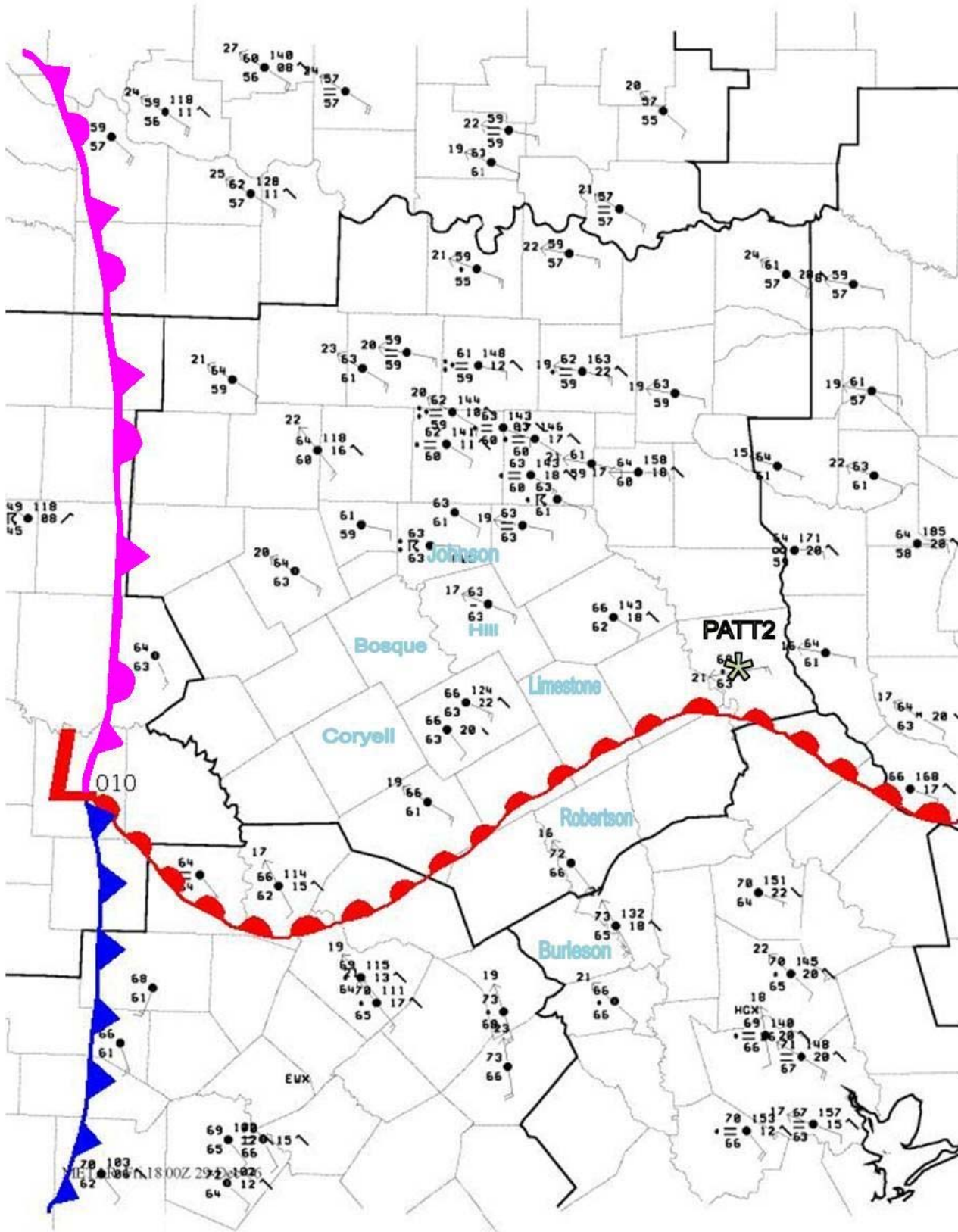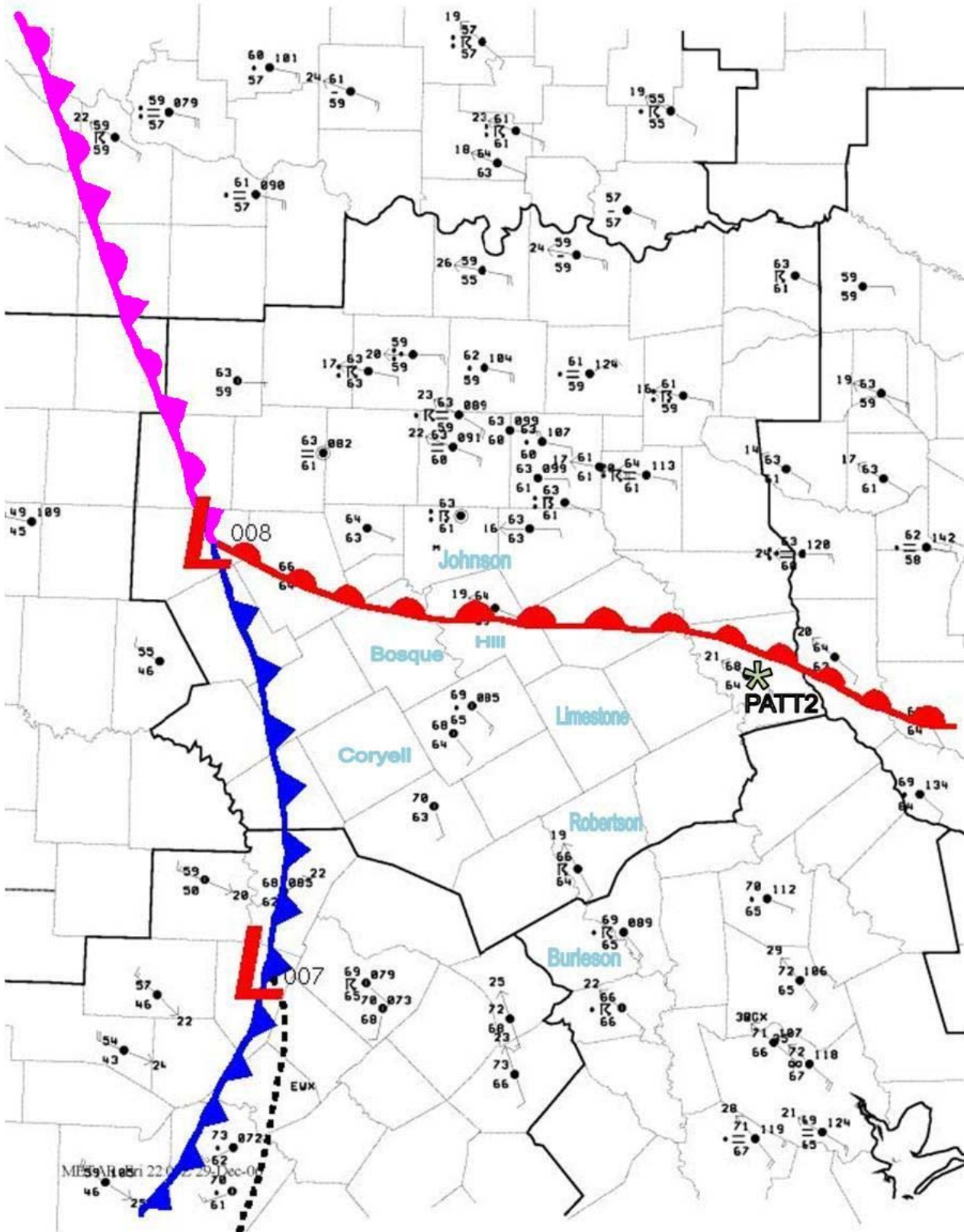
Fig. 17. Frontal analysis of 1800 UTC surface observations across Texas and southern Oklahoma. NWS WFO County Warning Areas are shown as bold black outlines with county boundaries shown as lighter gray lines. Selected county names are labeled in light blue text. Location of Palestine wind profiler (PATT2) labeled with light green asterisk.
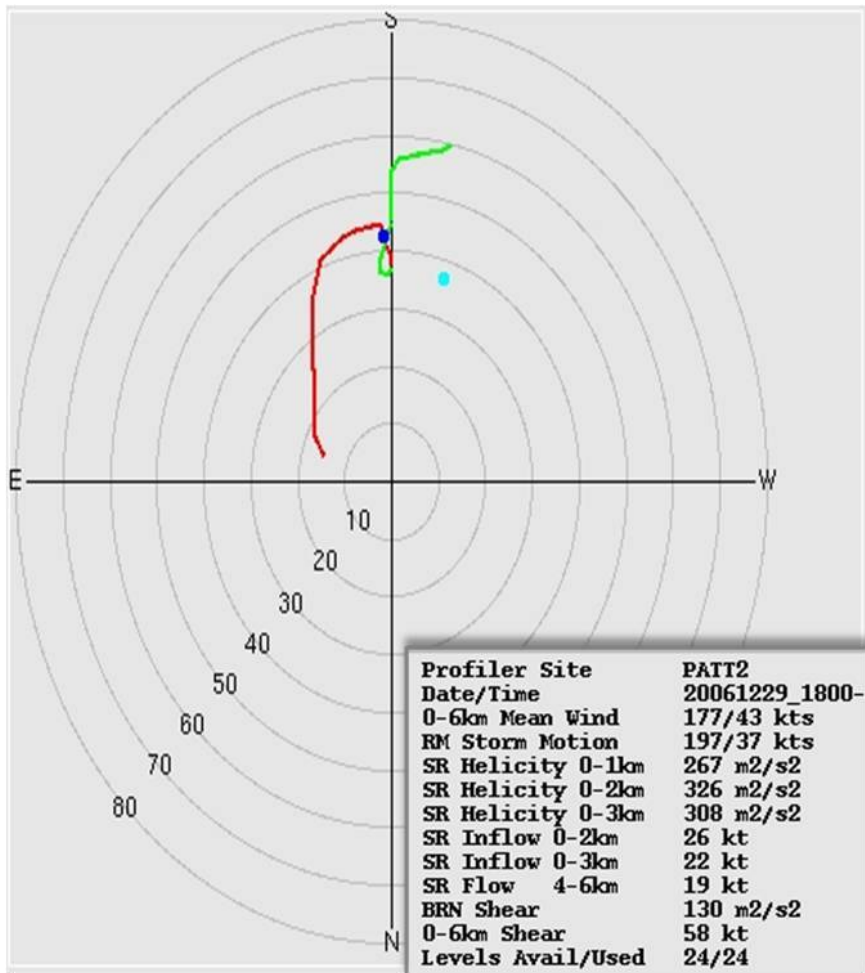
Fig. 18. 1800 UTC hodograph plot of 10 m - 6 km winds from the NOAA Profiler Network site at Palestine TX (PATT2). Gray labels depict wind speed magnitudes in knots. Winds at and below 3 km are plotted as red line segments and winds above 3 km are plotted as green line segments. Aqua-colored filled circle approximates a storm motion of a right-moving supercell; dark blue-colored filled circle approximates a motion of a cell moving to the left of the mean wind.
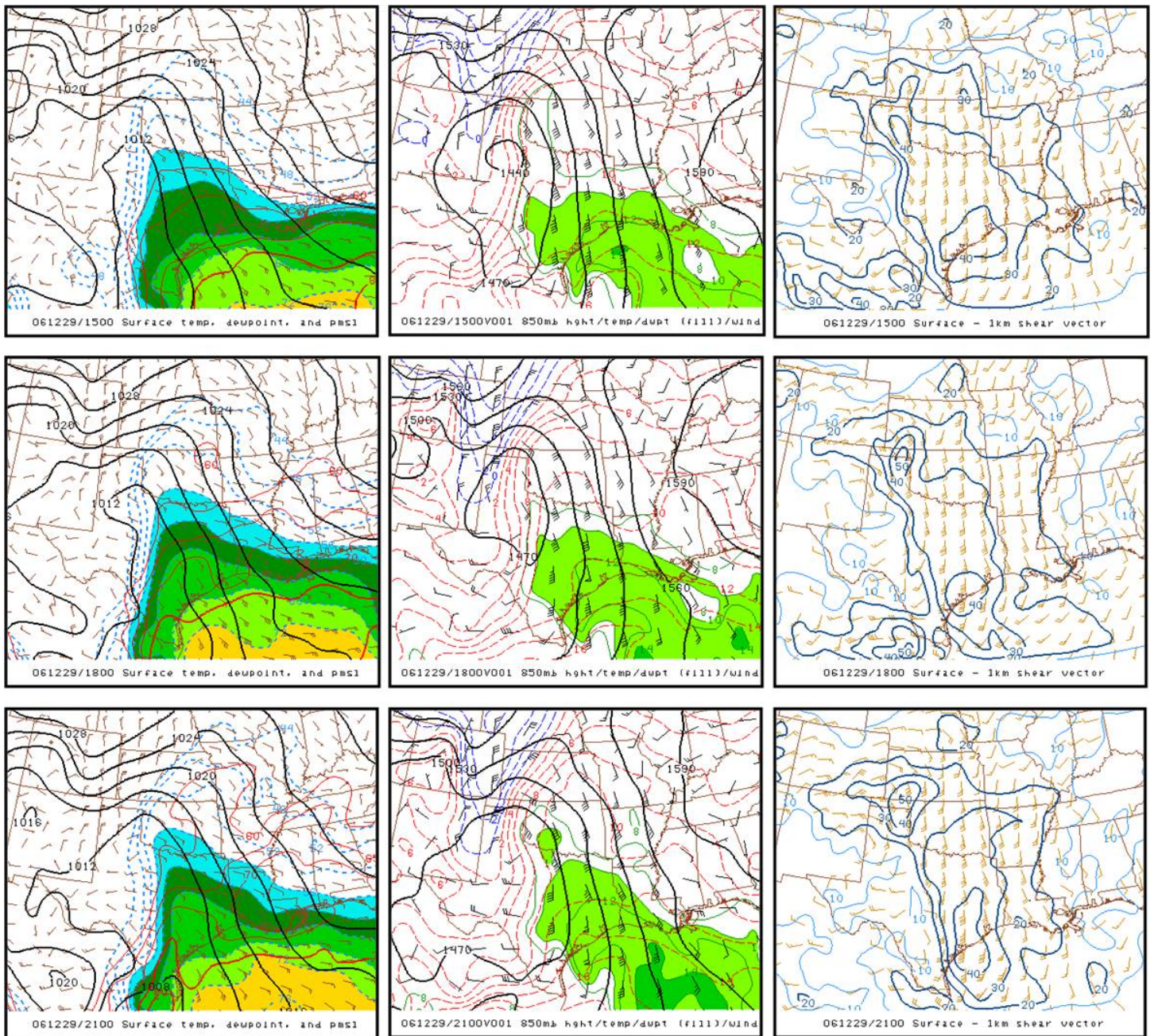
Fig. 19. Mesoanalysis graphics created by Storm Prediction Center (SPC) for 1500 UTC (top row), 1800 UTC (middle row) and 2100 UTC (bottom row) 29 December 2006. Left image in each row depicts isobars, surface wind barbs, surface isotherms (dashed, °F), and shading for surface dew points greater than 56° F. Middle images depict 850 hPa analyses of heights (solid, gpm), wind barbs, isotherms (dashed, °C), and shading for dew points greater than 10° C. Right images depict sfc – 1 km shear (knots) as wind barbs and blue contours at 10 kt intervals.

40

Fig. 20. Frontal analysis of 2200 UTC surface observations across Texas and southern Oklahoma. Selected county names are labeled in light blue text. Location of Palestine wind profiler (PATT2) labeled with light green asterisk. An expanding warm sector was analyzed across the southern third of the FWD CWA at this time with temperatures rising into the upper 60s °F to around 70 °F with dew points in the mid 60s °F.
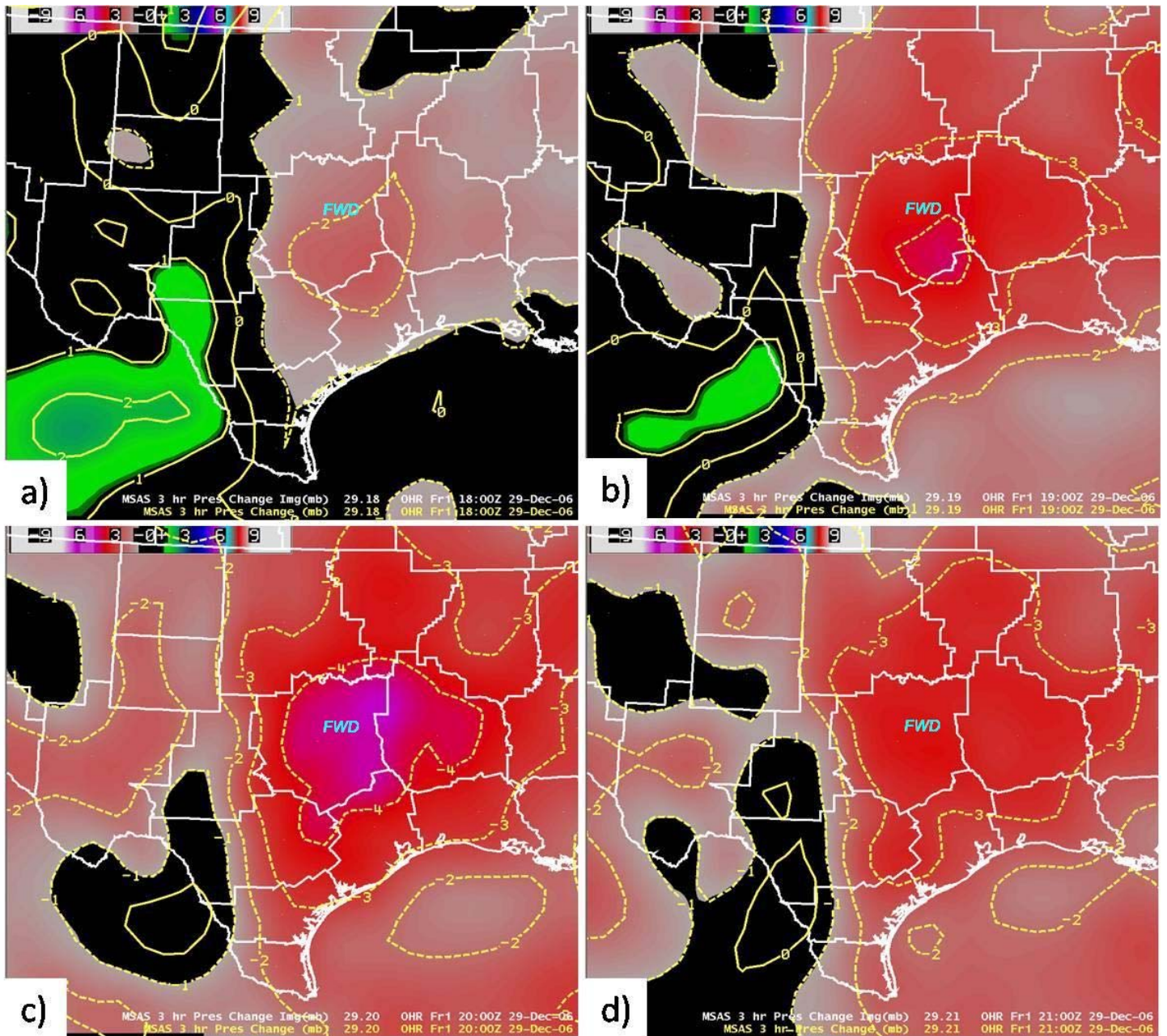
Fig. 21. Mesoscale Analysis and Prediction System Surface Assimilation System (MSAS) output from FWD Advanced Weather Interactive Processing System (AWIPS) depicting objective analyses of 3-h pressure changes. AWIPS Display 2-Dimension (D2D) output fields from MSAS are provided on a 60-km grid. Pressure change analysis for 3-h period ending at (a) 1800 UTC; (b) 1900 UTC; (c) 2000 UTC; and (d) 2100 UTC. In each image, solid white lines outline Weather Forecast Office County Warning Areas (FWD is labeled with light blue text); dashed yellow lines depict pressure falls at 1 hPa intervals and solid yellow lines depict pressure rises at 1 hPa intervals. Red and purple shading depicts pressure fall magnitudes greater than 1 hPa; green and blue shading depicts pressure rise magnitudes greater than 1 hPa.
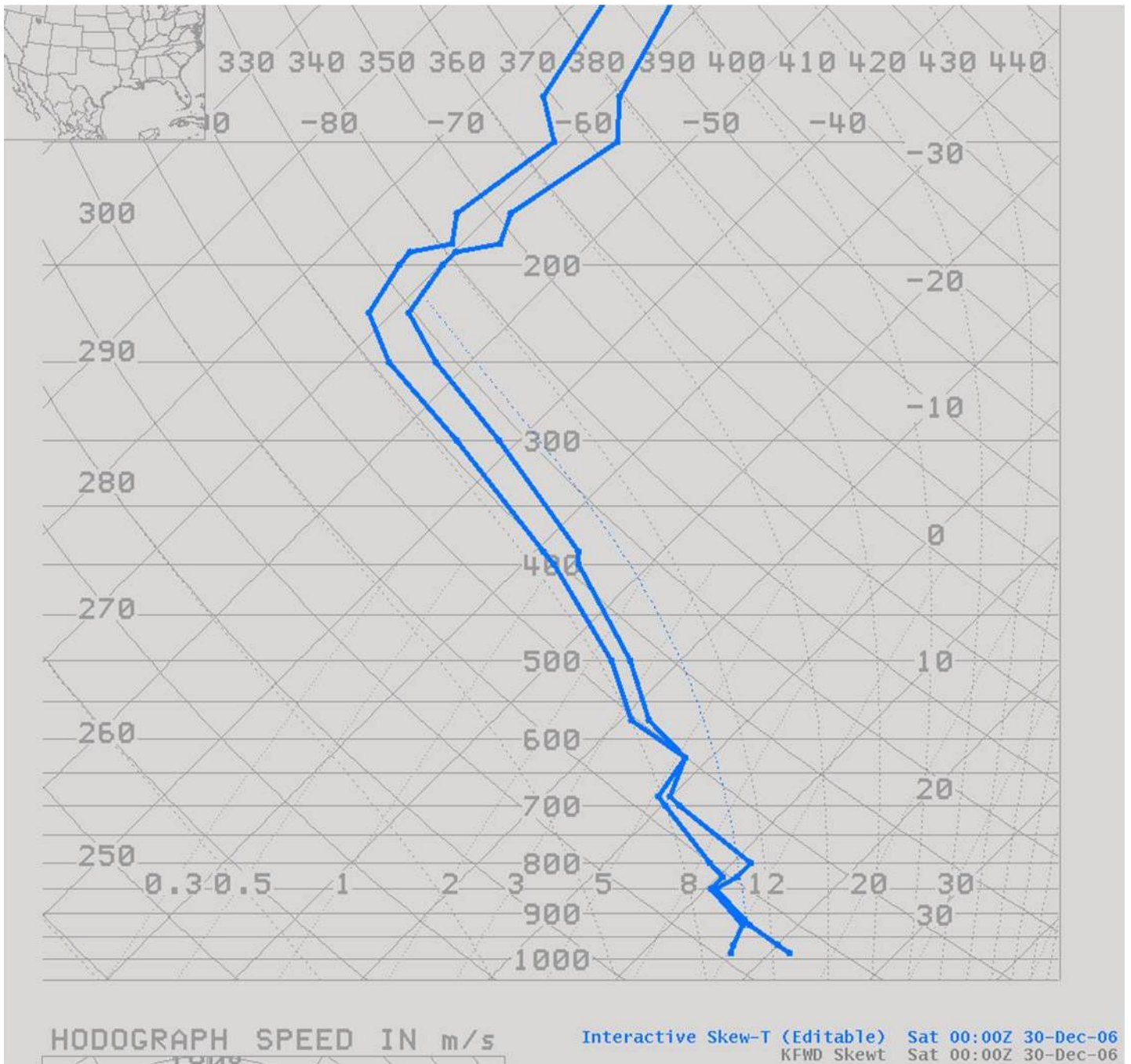
Fig. 22. Modified skew T-log P sounding from KFWD 0000 UTC 30 December 2006. Observed KFWD temperature and dew point sounding was modified to obtain a representative temperature and moisture profile of the environment near the tornadic outbreak region 100 km south of KFWD at 2000 UTC. The observed sounding was modified based on a surface temperature of 70°F and a surface dew point temperature of 63°F. Thermodynamic parameters derived from this modified sounding are given in Table 4.
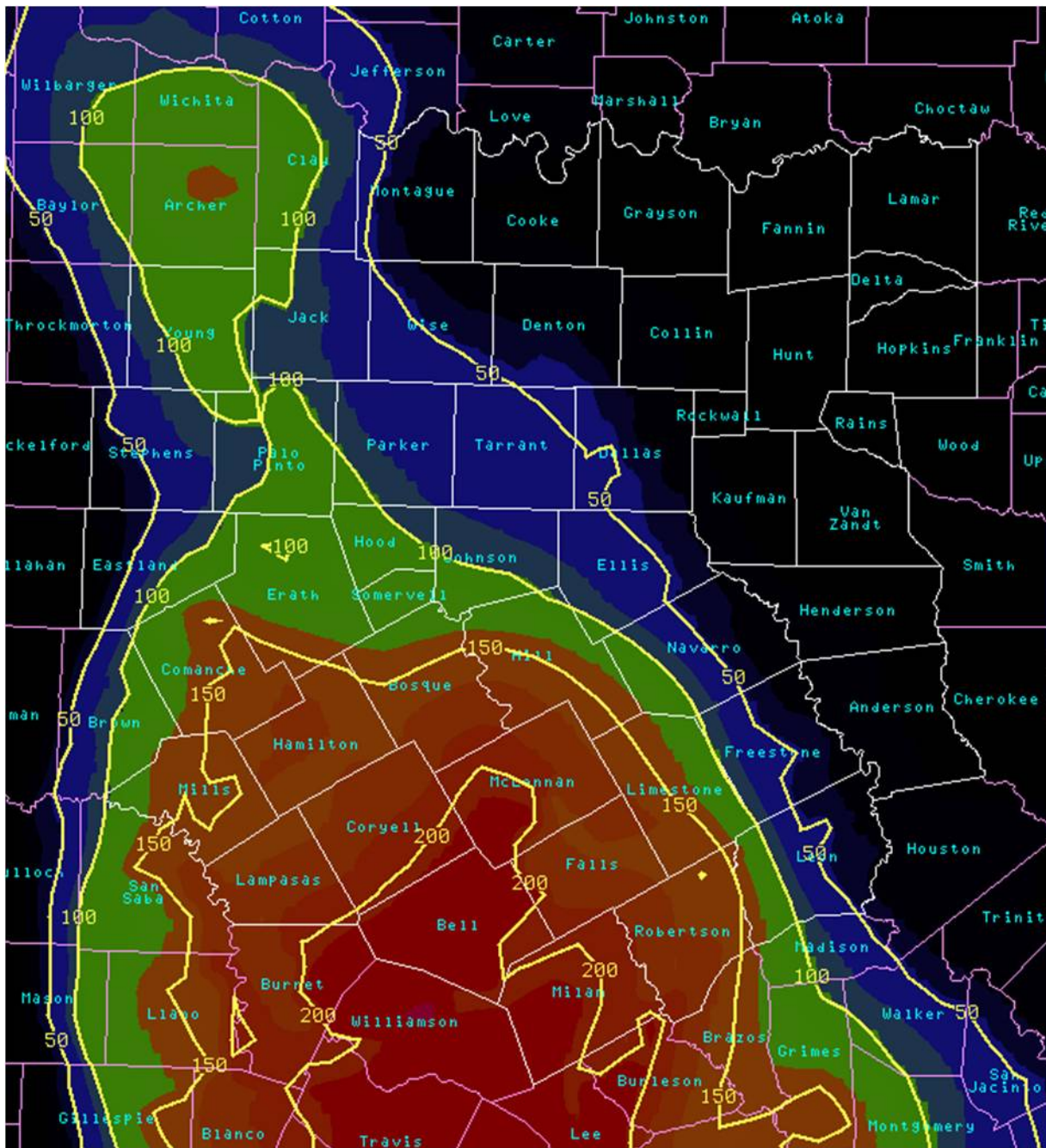
Fig. 23. Local Analysis and Prediction System (LAPS; see Albers et al. 1996, and McGinley 1995) analysis of sfc-3 km CAPE (solid, J kg^{-1}) at 2000 UTC 29 December 2006 across northern Texas. Color shading indicates values progressively in excess of 50 J kg^{-1}.
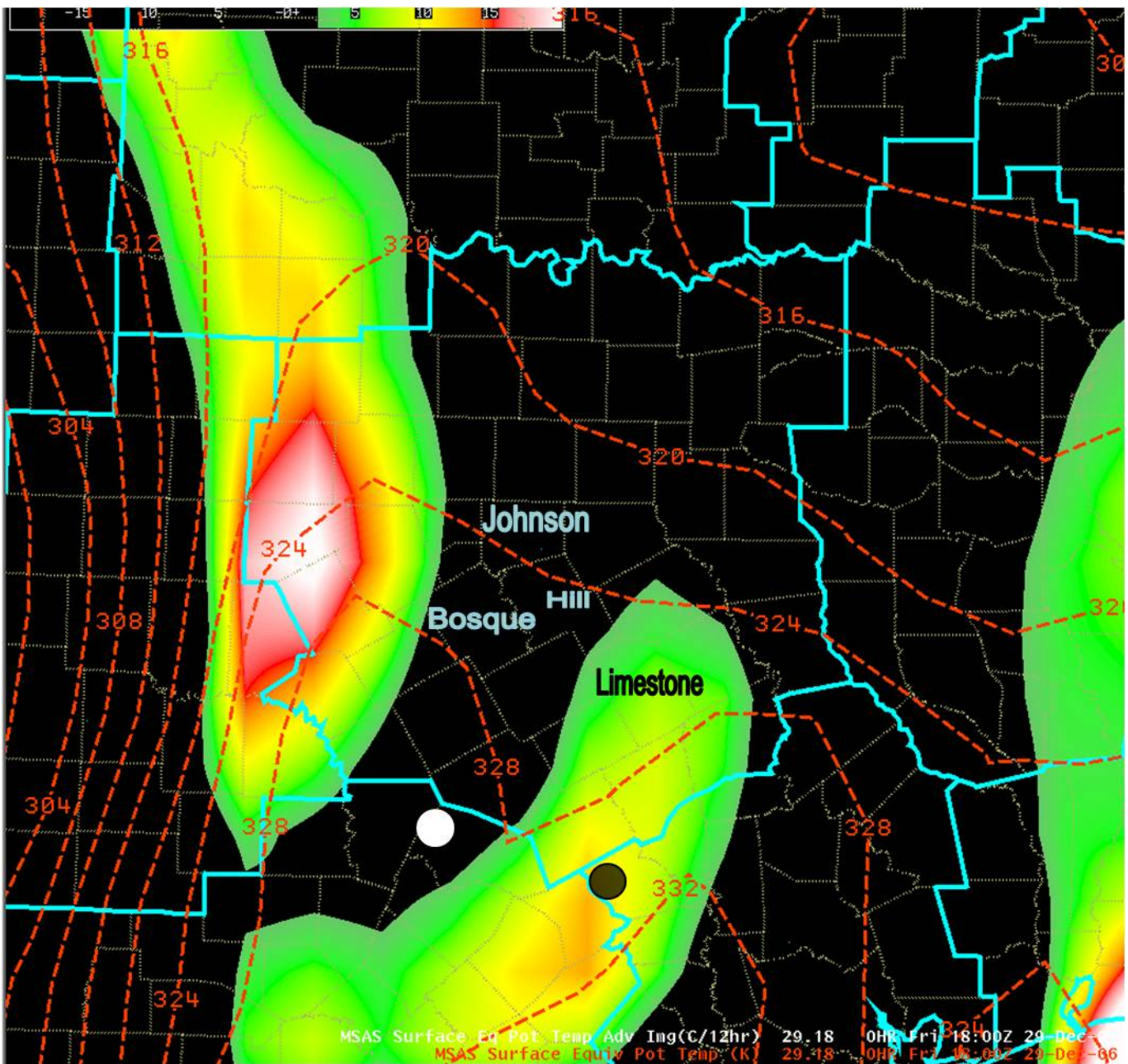
**Fig. 24.** MSAS objective analysis of surface Θ_e (dashed, K) and positive values of surface Θ_e advection (shading, °C [12 h]$^{-1}$) at 1800 UTC 29 December 2006. Maxima in advection were analyzed across the western part of the FWD CWA, just east of the occluded front, and in the southern part of the FWD CWA to the northwest of a second Θ_e ridge. The large white dot represents the initiation region of a thunderstorm that eventually became supercellular and produced F2 tornadoes in Bosque, Hill, and Johnson Counties. The large black dot represents the initiation region of a thunderstorm that evolved into a supercell that produced an F2 tornado in Limestone County. Both storms initiated between 1800 UTC and 1900 UTC.
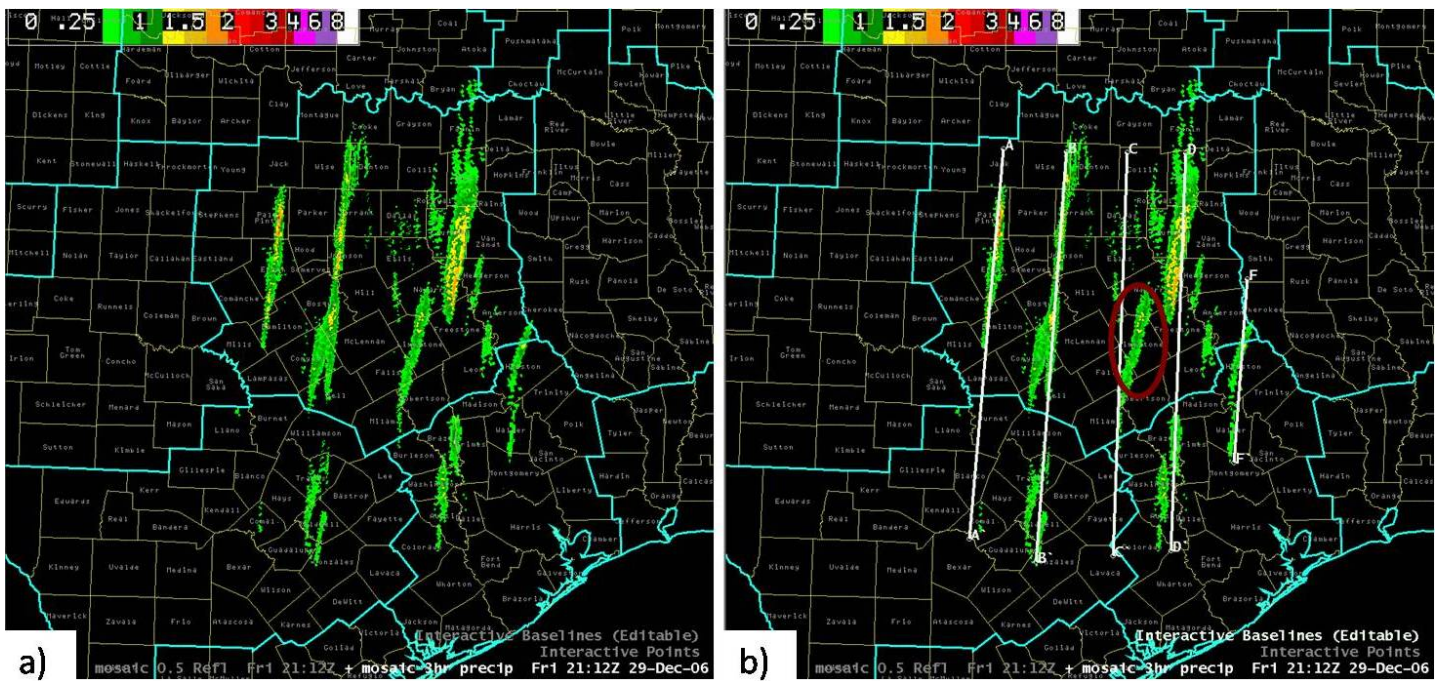
Fig. 25. Illustration of convective organization into several distinct north-south oriented clusters during the 29 December 2006 outbreak. (a) AWIPS D2D mosaic of radar-estimated precipitation for the 3-h period ending at 2100 UTC. The lightest green color represents radar rainfall estimates of 12.7 mm (0.5 in), with darker green and yellow colors corresponding to 25 – 37 mm (1.0 - 1.5 in) estimates; (b) Same as (a), but with several subjectively drawn lines (labeled A, B, C, D and F) representing approximate locations of bands of maximum rainfall for the 3-h period. Average horizontal spacing between the 5 bands is 70 km. The green colors highlighted in the red oval to the right of Line C across Falls, Limestone and Navarro Counties resulted from a supercell thunderstorm that originated close to Line C in Milam County, but then exhibited a storm motion to the right of the mean wind.
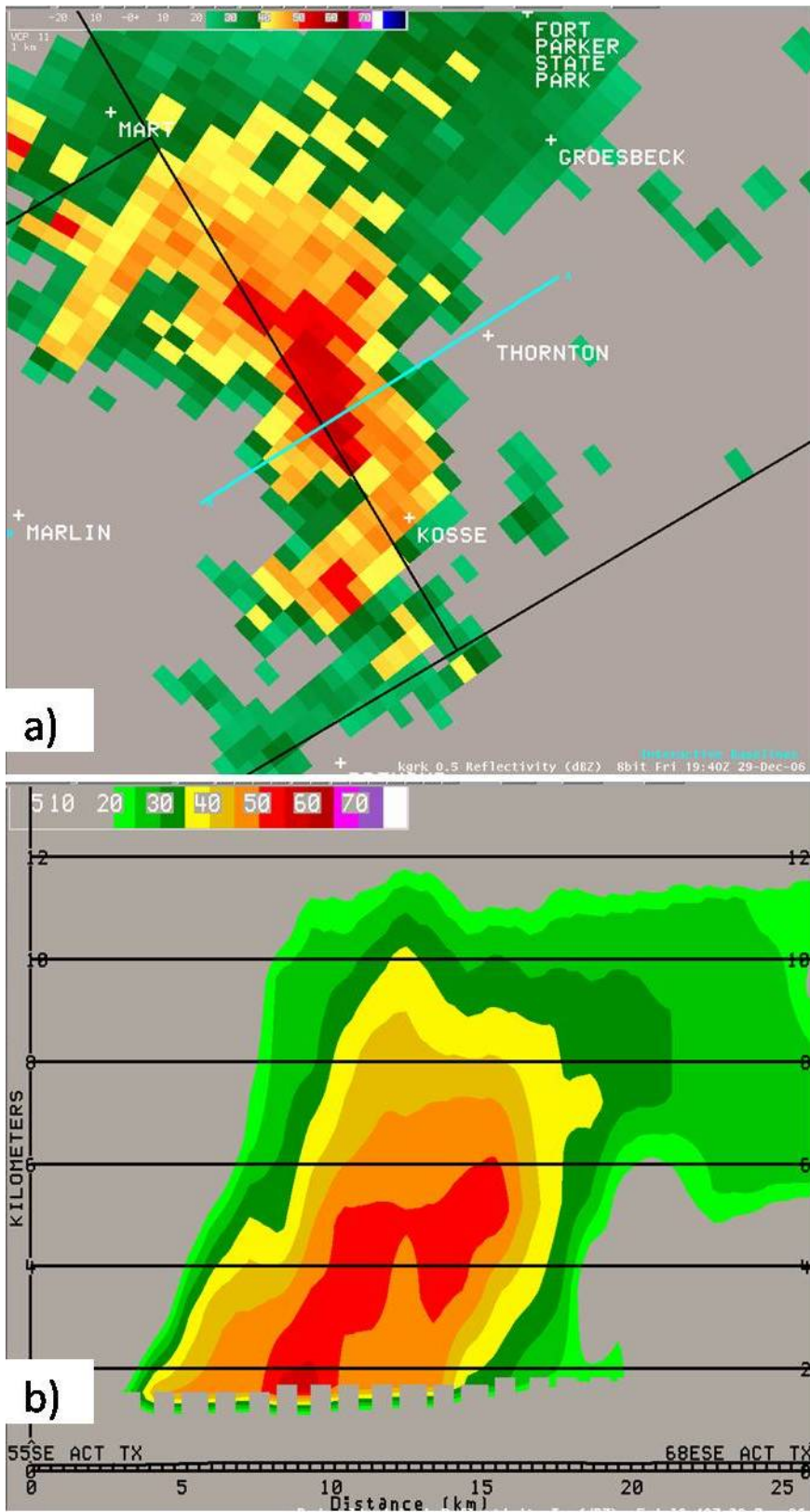
Fig. 26. KGRK WSR-88D depiction of bounded weak echo region (BWER) of Limestone County supercell at 1940 UTC 29 December 2006. (a) 0.5° base reflectivity. Solid black lines depict county outlines. City names and locations are shown in white text. Light blue line depicts location of reflectivity cross section. (b) Reflectivity cross-section image showing evidence of a BWER centered near 4 km height at approximately 13 km on the horizontal scale.
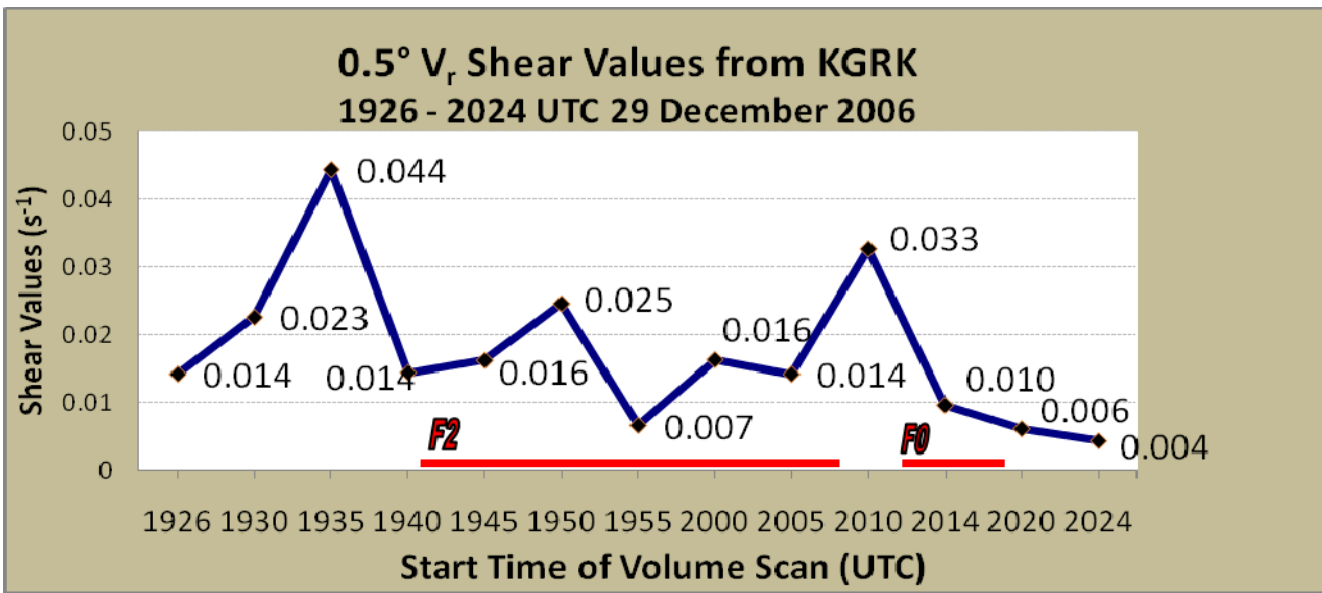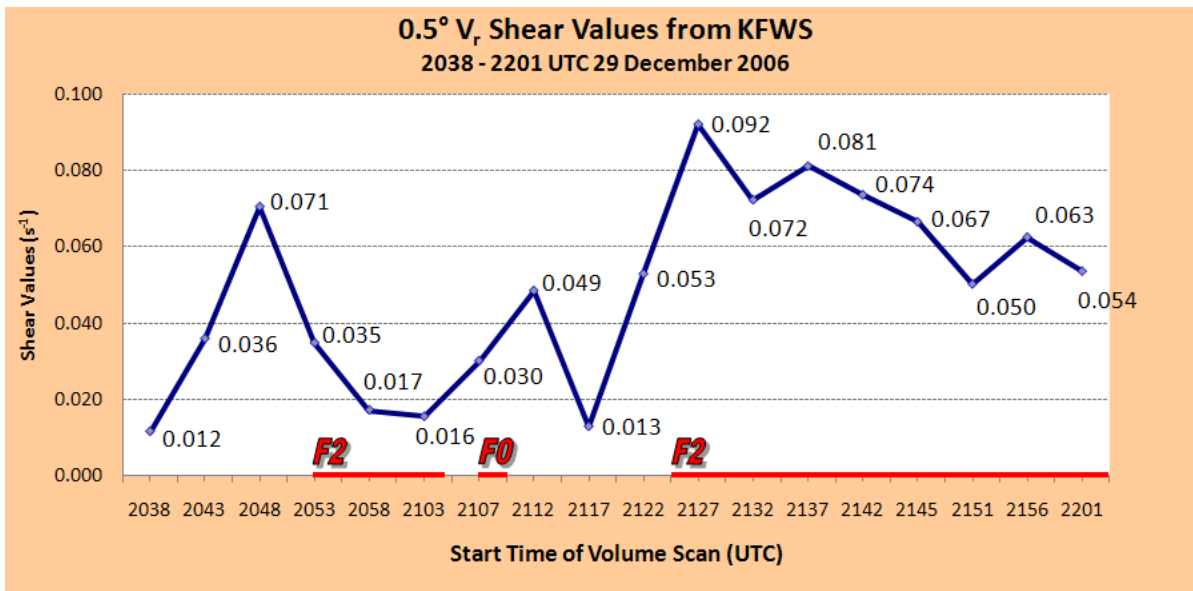
Fig. 27. Trends in 0.5° rotational shear of the Limestone County supercell as output by WSR-88D algorithm from KGRK between 1926 UTC and 2024 UTC 29 December 2006. Tornado occurrence times and associated tornado ratings are designated by red lines and text. Note that tornadoes were reported after each peak in the shear values. It can also be seen that shear values remained at higher values overall for the stronger F2 versus the weaker F0 tornado.
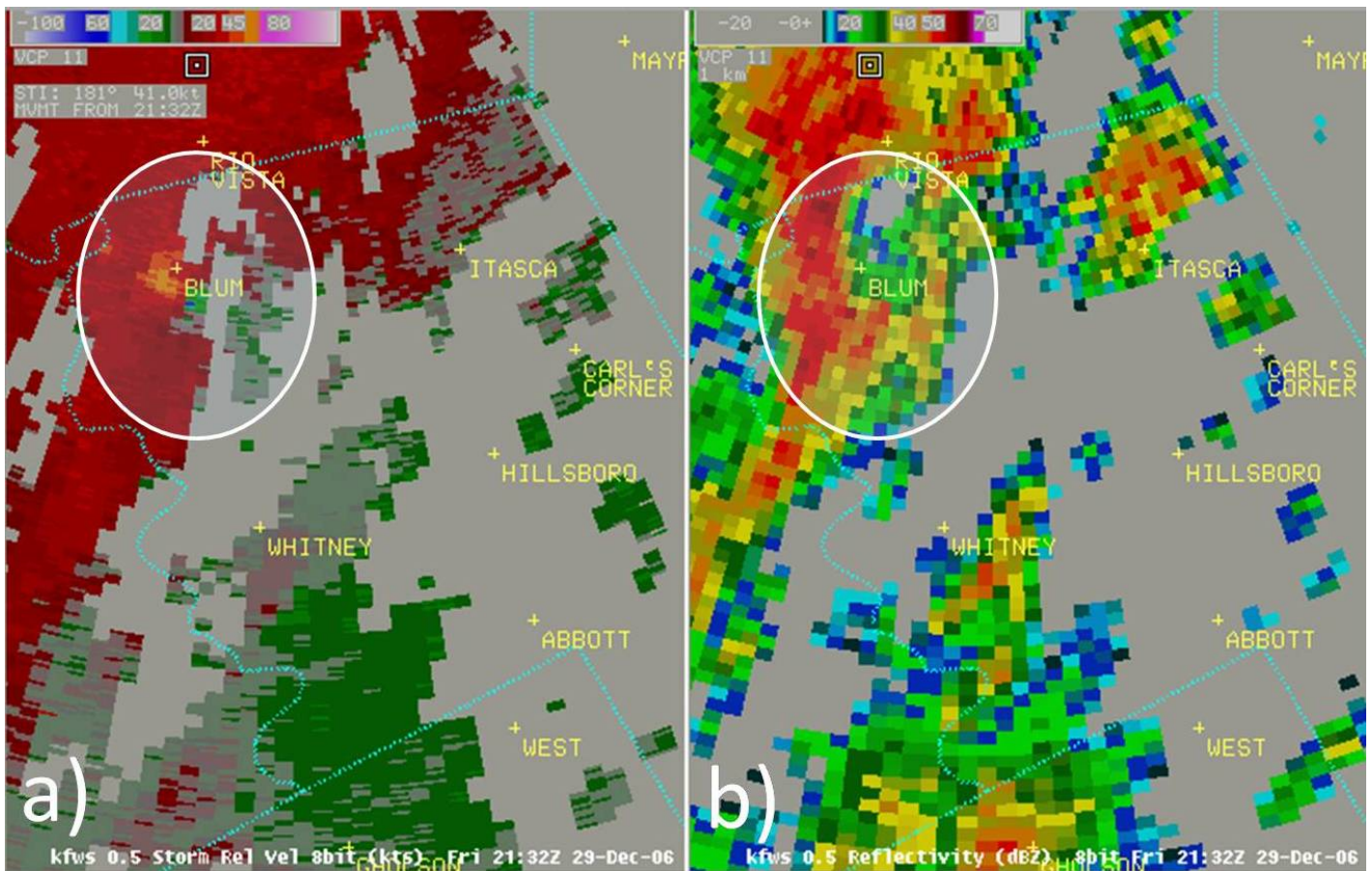
Fig. 28. Tornadic supercell thunderstorm near Blum, Texas (northwest Hill County), as depicted by KFWS at 2132 UTC 29 December 2006 when an F2 tornado was occurring. KFWS is approximately 35 km to the north of the supercell at this time. (a) 0.5° Storm-relative mean radial velocity (SRM); (b) 0.5° reflectivity.
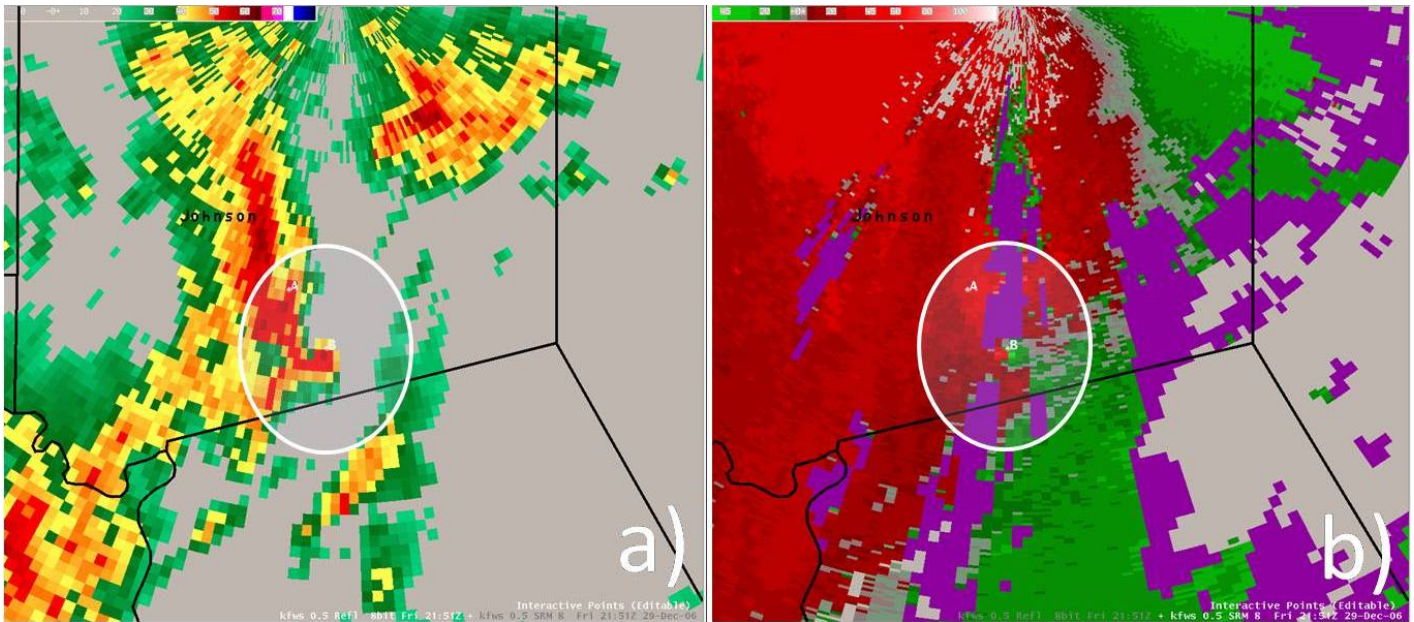
Fig. 29. KFWS WSR-88D imagery showing tornadic supercell at 2151 UTC 29 December 2006 when an F2 tornado was occurring. KFWS is approximately 25 km (15.5 mi) to the north of the supercell at this time. Black lines depict county outlines. Johnson County is labeled in black text. (a) 0.5° base reflectivity image. Note the well-defined hook echo (center of white circled region) associated with the supercell in far southern Johnson County. (b) 0.5° storm-relative mean radial velocity (SRM) image. Note the gate-to-gate cyclonic circulation (near center of white circled region) denoting existence of intense small-scale rotation associated with the supercell.

Fig. 30. Trends in 0.5° rotational shear of a family of supercells as output by WSR-88D algorithm from KFWS between 2038 UTC and 2201 UTC 29 December 2006. The supercells affected parts of Bosque, Hill, and Johnson Counties during this time period. Tornado occurrence times and associated tornado ratings are designated by red lines and text. Note that F2 tornadoes were reported near the time of or shortly after each peak in the shear values.

Table 1: Statistics for tornado events and county-based tornado warnings issued by WFO FWD on 29 December 2006.

Tornado Warnings Issued	36	Tornado Events	23
Tornado Warnings verified by tornado	14	Tornadoes warned by Tornado Warning	21
Tornado Warnings not verified by tornado	22	Probability of Detection (POD) for Tornado Warnings	.913
False Alarm Ratio (FAR) for Tornado Warnings	.611	Ave lead time for Tornado Events (min)	12.8

Table 2: Summary of the tornadoes across north Texas
on 29 December 2006 that were rated F2. (NCDC 2007)

County	Path Length (miles)	Avg. Width (yards)	Deaths	Injuries	Damage (million dollars)
Limestone	20	400	1	20	1.0
Bosque	7	300	0	0	0.4
Hill & Johnson	23	250	0	12	2.5

Table 3: Parameters from the sounding observations taken at 1200 UTC 29 December 2006
at Fort Worth, TX (KFWD) and Corpus Christi, TX (KCRP).

1200 UTC 29 December 2006 Observed Sounding Parameters	KFWD	KCRP
700 - 300 hPa Lapse Rate	8.2 C km^{-1}	8.2 C km^{-1}
Precipitable Water	27.7 mm (1.09 in)	23.6 mm (0.93 in)
Mean mixing ratio (sfc – 850 hPa)	9.2 g kg^{-1}	12.0 g kg^{-1}
Surface Based CAPE	0 J kg^{-1}	1000 J kg^{-1}
Bulk Shear 10 m – 1 km	15 m s^{-1} (30 kt)	14 m s^{-1} (27 kt)
Bulk Shear 10 m – 6 km	21 m s^{-1} (41 kt)	20 m s^{-1} (38 kt)

Table 4: Parameters from the modified rawinsonde observation taken at 0000 UTC 30 December 2006 at Fort Worth, TX (KFWD). Figure 22 shows the modified skew-T diagram; modifications included adjustments to low-level temperatures and mixing ratios with no adjustments to wind. The thermodynamic adjustments were intended to better represent the environment in the warm sector 100 km south of KFWD. All parcel-based parameters in this table are based on lifting a surface-based parcel.

KFWD Modified Sounding Parameters	0000 UTC 30 Dec 2006
SBCAPE	1276 J kg^{-1}
SBCIN	-3 J kg^{-1}
Sfc – 3 km SBCAPE	117 J kg^{-1}
700 – 300 mb Lapse Rate	6.8 C km^{-1}
Mean Mixing Ratio (sfc – 850 hPa)	11.0 g kg^{-1}
Precipitable Water	37.8 mm (1.49 in)
LCL height	655 m AGL (2575 feet MSL)
EL height	11.6 km MSL (38 kft)
Bulk Shear 10 m - 1 km	16 m s^{-1} (32 kt)
Bulk Shear 10 m - 6 km	26 m s^{-1} (51 kt)
Storm-Relative Helicity 10 m - 1 km	312 m^2 s^{-2}
Storm-Relative Helicity 10 m – 3 km	506 m^2 s^{-2}
Energy-Helicity Index (using 10 m – 1 km SRH)	2.5
Energy-Helicity Index (using 10 m – 3 km SRH)	4.0
Vorticity Generation Parameter	0.22 m s^{-2}